The Retrieval of Leaf Inclination Angle and Leaf Area Index in Maize

Fang Fang

June, 2015

Course Title:	Geo-Information Science and Earth Observation for Environmental Modelling and Management
Level:	Master of Science (MSc)
Course Duration:	September 2013 – June 2015
Consortium partners:	Lund University (Sweden) Faculty ITC, University of Twente (The Netherlands)

The Retrieval of Leaf Inclination Angle and Leaf Area Index in Maize

By

Fang Fang

Thesis submitted to the Faculty of Geo-Information Science and Earth Observation of the University of Twente in partial fulfilment of the requirements for the degree of Master of Science in Geo-information Science and Earth Observation, Specialization: Environmental Modelling and Management.

Thesis Assessment Board

External Examiner	Dr. J. Clevers (University of Wageningen)
Chair	Prof. Dr. Andrew K. Skidmore
First Supervisor	Ing. Valentijn Venus, MSc
Second Supervisor	Prof. Dr Wout Verhoef

UNIVERSITY OF TWENTE.

FACULTY OF GEO-INFORMATION SCIENCE AND EARTH OBSERVATION

Disclaimer

This document describes work undertaken as part of a programme of study at the Faculty of Geo-Information Science and Earth Observation of the University of Twente. All views and opinions expressed therein remain the sole responsibility of the author, and do not necessarily represent those of the institution.

Abstract

Leaf area index (LAI) and leaf inclination angle distribution (LAD) are two important variables that characterize vegetation canopy structure, and play a key role in water, gas and energy exchange between canopy and atmosphere. They serve as main inputs of models that simulate photosynthesis, evapotranspiration and radiative reflectance. Ground measurements of LAI are often conducted with instruments based on optical theory using the gap fraction model. To use the model, LAD has to be quantified first. However, LAD in reality is complex and varies among/within species and growing stages, making it difficult to be quantified. Leaf angle distribution functions (LIDFs), a mathematic description of LAD, have been developed to approximate LAD and simplify the calculation, but the common assumed LIDFs depart from real canopy and introduce certain amounts of errors in LAI retrieval. Additionally, the field measurement of LAD using conventional methods is labor intensive and time consuming. This study aims to: (1) investigate the LAD variation of maize canopy at different developing stages and environmental conditions as well as its influence on maize reflectance; (2) quantify the LAI retrieval error of using different LIDFs and find the LIDF that best fits maize plant LAD at each developing stages, and (3) improve a newly developed digital photographic (DP) method to measure maize plant LAD with reliability and higher efficiency.

The study finds that LAD of maize plant at vegetative and reproductive stages is subject to plagiophile canopy type. Maize plants at the same growing stage but grown under different environmental conditions have an identical LAD type ($P>0.29$). Planophile type canopy was observed in this study. This had never been reported for maize before. Planophile canopy type has higher reflectance than plagiophile type regardless of LAI level. In addition, planophile canopy also leads to a higher NDVI value.

Furthermore, two-parametric LIDF, beta distribution and trigonometric function, outperformed the other LIDFs in characterizing maize plant LAD and LAI retrieval. The solution-improved trigonometric function gives the best fit and yields the smallest fitting and the lowest LAI retrieval error.

The Anderson-Darling test result shows no significant difference exists between the DP method and manual measurement ($P>0.61$). The LAI retrieved using LAD from both methods at a viewing angle 57° shows good agreement. The minimum sample size was determined using the bootstrap technique, and the result indicates that 15 plants (113 leaves) are needed to achieve a reasonably good and reproducible LAD result.

The LAD of maize plant does not vary significantly at vegetative and reproductive stages, and can be described as plagiophile canopy. However, planophile canopy also occurs in maize canopy and results in higher reflectance than plagiophile canopy, which one needs to be aware of when using remote sensing data to study vegetation. Trigonometric function is recommended to simulate vegetation canopy due to its good and robust performance. The LAI retrieval error remains negligible when using parametric LIDF or non-parametric LIDF that is closest to LAD. Therefore, LAI can be

retrieved with high accuracy using parametric LIDF or reasonably assumed non-parametric LIDF (the assumed LIDF should be close to the real LAD). The adjusted DP method allows for more efficiency and flexibility to measure LAD. Since the DP method could be easily incorporated into a smartphone platform, there is big potential and opportunity ahead for sampling LAD and in turn LAI using smartphones.

Key words: leaf inclination angle distribution, leaf area index, LAI, digital photographic method

Acknowledgement

I would like to thank my supervisors Venus Valentijn and Wout Verhoef for their guidance and kind support during the thesis journey. The meetings with Venus were full of ideas bridging scientific research and practical social impacts, which leads me to keep innovative thinking. This has opened a door for me. Sometime when I encounter a research problem, I would look at it in a different perspective. I am inspired and motivated by his broad vision and rich knowledge about different fields. I want to express my sincere thanks to Wout. It is my privilege to work with him. He has been supportive and helpful during the entire thesis work. Especially on leaf angle distribution function part, he has helped me understand it better and encouraged me to explore the potential influence on reflectance, which brought the research work into depth to some degree. He always strikes points clearly and fast, and all discussions during the meeting have been fruitful for me. The way that he tackles problems has set up a very good example for me. I am inspired by the richness of his PhD thesis and the power of SLC model. All those insightful talks make me think and reflect.

The field work was conducted on a farm with kind support from Harry, Bernadette, their daughter and colleague. I want to thank them for allowing us to do the field data collection on their farm and for their hospitality. It is so much appreciated that they offered us ride to the bus stop so many times as well as all kinds of help. The field work became full of joy because of their generosity and kindness. I want to thank my colleage Richard Makanza for support and great cooperation during the field work.

I would like to thank Yu Zhou, Anniux Maldonado and Matthew Bruno for their valuable advice on improving the manuscript.

I am grateful to the GEM program for providing this interesting MSc course where science and technology meet and integrated, where research and application are connected as well as a multi-cultural atmosphere. All the teaching staff and supporting staff are thanked and appreciated for broadening my knowledge and skills and ensuring quality study. I want to thank all GEM colleagues for those precious times together, especially Hadi, who is supportive and always being a solution seeker. I would like to thank Lund and ITC friends, especially Rakhat Asankozhoeva, Analia Guachalla Terrazas, Anniux Maldonado, Kavita Salvi, Maria angela dissegna orduna, Gunjan Pranay Sharma and Xinyi Dai, for making an international family for me.

Finally, I would like to thank my families, for their support.

Table of Contents

List of Figures

List of Tables

1. Introduction

1.1 Background

Leaf area index (LAI) is defined as half the total developed area of leaves per unit ground horizontal surface area (Chen & Black, 1991). It is a widely used biophysical variable in forest and agriculture research. LAI indicates the greenness of canopy and in turn light interception by the canopy, and thus is very important for estimating photosynthesis. It drives canopy microclimate, and controls water and gas exchange occur at the leaf surface, which also contribute to evapotranspiration estimate (M. Weiss, Baret, Smith, Jonckheere, & Coppin, 2004). Therefore, it is an important component of biogeochemical circles in ecosystem (Bréda, 2003). Physical process based radiative transfer model (Verhoef & Bach, 2007) and ecosystem model such as dynamic vegetation growth model (Smith, Knorr, Widlowski, Pinty, & Gobron, 2008) often employ LAI as an important input/output parameter to perform better quantitative simulations. LAI is also one of the essential crop variables (ECVs) that characterize the crop growth condition, and the hyper temporal monitoring of LAI allow the farmers and scientists better understand and estimate the crop growth development and yield (Haboudane, 2004). Hence, many studies have been done during the past decades to retrieval LAI using different methods and based on different theories in both large scale level or ground measurement level.

1.1.1 LAI

Statistical model using satellite or airborne images is one of the most widely used methods to estimate LAI in large scale. Usually the images are composed of multiple spectra bands or even hyper spectra bands and LAI is estimated using vegetation index (VI) derived from the bands. VI is arithmetic operations of selected bands, and is often obtained though regression to find the bands highly correlated with LAI. Massive VI have been proposed (Broge & Leblanc, 2001; Zheng & Moskal, 2009). However, the performance of each VI depends on environmental conditions, and there are always limitations. One major problem is the saturation of LAI. VI cannot predict the level out behavior of LAI (Darvishzadeh et al., 2008; Haboudane, 2004). In addition, the chlorophyll content affects the LAI estimates and it is difficult to exclude the influence (Haboudane, 2004). Some researchers found that the image derived LAI is site specific and is affected by sampling condition as well (Bréda, 2003; Darvishzadeh et al., 2008). The above mentioned problems do not exist in physical models.

Physical process based models are built on the relationship between spectra and canopy architecture, biophysical and biochemical parameters. The simulated spectra takes into account the interaction between penetrating light and vegetation canopy as well as soil surface through physical laws. Therefore, they can be applied universally (Rex, 2010). To retrieve those parameters from the physical models, inversion technique is used. The simulated spectra and the measured one were compared, and the parameters from the most similar simulated spectra are assumed to be the parameters of the measured. Some models have been demonstrated to achieve good LAI estimation (Frédéric Baret et al., 2007; Propastin & Panferov, 2013). However, the disadvantage of using a

physical model is ill-posedness during inversion, which means several parameter sets (including both the correct and incorrect ones) may generate identical simulated spectra and the wrong set may be picked.

Above all, those two methods often require ground measurement as a reference for assessment. Field measurement is considered to provide more accurate result that often serves as LAI ground truth. It is usually used to validate the above methods. There are two categories of ground measurement methods: direct methods and indirect methods (Norman and Campbell, 1989, Breda 2003, Weiss 2004). The direct (including semi-direct) methods include: harvesting, allometric relationship, litter collection and needle technique (Bréda, 2003). They provide the access to measure leaf area directly and the reference to evaluate indirect methods. However, limitations are also seen in these methods: harvesting is destructive and only suitable for vegetation of small structure; allometric relationship method is site and species specific, and also year-dependent; Litter collection is widely used in forest ecology and serves as a reference, but again it varies with a lot factors; Needle technique requires an intensive sampling to quantify an average contact number and LAI. These direct methods are labor intensive and time consuming (M. Weiss et al., 2004). Thus indirect methods have been developed to study canopy structure since 1960s.

The indirect methods retrieve LAI by measuring radiation transmittance through canopy using radiative transfer theories (Bréda, 2003). These are non-destructive methods and based on a statistical consideration of foliage element distribution (namely leaf angle distribution LAD) in the canopy. These methods estimate the contact frequency or the gap fraction. The gap fraction method is preferred since contact frequency is difficult to measure in a representative way (M. Weiss et al., 2004). The radiation penetrating through canopies can be expressed by Beer-Lambert law that attenuation of radiation is proportional to the optical distance inside the medium. It assumes that the leaves have random spatial distribution and the leaves are small compared to the whole canopy. When the assumption is satisfied, measuring gap fraction is equivalent to measuring transmittance (Bréda, 2003; M. Weiss et al., 2004). Nilson (1971) found that gap fraction $P_0(\theta,\phi)$ in direction (θ,ϕ) is an exponential function of LAI even when the above assumptions are not fulfilled (M. Weiss et al., 2004), and it can be expressed using the Poisson model (eq.1.1). A modified version of Poisson is proposed to take into account the clumping effect of leaf arrangements, and is known as Markov model (Nilson, 1971; M. Weiss et al., 2004) shown in eq.1.2.

$$P_0(\theta,\phi) = \exp(\frac{-G(\theta,\phi)L}{\cos(\theta,\phi)}) \tag{1.1}$$

$$P_0(\theta,\phi) = \exp(\frac{-\lambda_0 G(\theta,\phi)L}{\cos(\theta,\phi)}) \tag{1.2}$$

$$I = I_0 \exp(-KL) \tag{1.3}$$

Where L stands for LAI, $G(\theta,\phi)$ the project function and λ_0 the clumping index. $G(\theta,\phi)$ is defined as the mean projection of a unit leaf area, and depends on leaf inclination angle distribution function (LIDF). $G(\theta,\phi)/\cos(\theta,\phi)$ is the extinction coefficient K. The clumping index λ_0 takes into account the clumping effects of leaves. LAI could be obtained through inversing the model.

Gap fraction based LAI measurement methods are widely used for its simplicity. sunSCAN (Delta T Devices Ltd, Cambridege, UK), AccuPAR (Decagon Device, Pullman USA), LAI2000 (Li-Cor, Lincoln, Nebraska, USA) and Demon (CSIRO, Canberra, Australia) (Bréda, 2003) were developed based on this optical radiation theory to derive structural canopy variables. During the measurement, both above canopy and under canopy radiation are measured and thus transmittance is obtained though taking the ratio of the two values (eq.1.3). These instruments, however, are usually expensive and have a low portability, and require long time maintenance services in case of damages (Confalonieri et al., 2013). In addition, they have to be used in certain illumination conditions to obtain correct LAI result (Bréda, 2003).

Hemispherical photography or fish-eye photography has long been used to study canopy structure (Bréda, 2003). Thanks to the recent technological development, high spatial and radiometric resolution cameras have become increasing affordable (Liu, Pattey, & Admiral, 2013). In addition the advances in digital image processing software allow the image analysis to be more powerful and efficient. All these lead to a renewal of interest in digital hemispherical photography (DHP) oriented methods (Bréda, 2003). Other than DHP, the photographs taken using rectilinear lens also becomes research interest (F. Baret, de Solan, Lopez-Lozano, Ma, & Weiss, 2010; Liu et al., 2013; Ryu et al., 2010; Sandmann, Graefe, & Feller, 2013). Both methods measure gap fraction from the photos through classifying green part and the sky.

The same trend is seen in smartphone application. The integrated sensors such as camera, compass, inclinometer and GPS within the smartphone and the advanced computation capabilities and increasing storage memories all make it suitable for scientific orientated applications. Besides, it has high portability and easy interface, and is affordable, which leads to its high potential to assist scientific studies. Recently, there are studies on LAI sampling app development on smartphone platforms (Confalonieri et al., 2013). This smartphone oriented LAI measurement allows for the possibility of monitoring crop with high temporal resolution. Besides, it has the potential to allow for the general public involvement and contribution to science activities easily by collecting field data using a smartphone app. This shows promising future of smartphone apps for scientific purpose.

1.1.2 Leaf inclination angle distribution (LAD)

LAD itself is an important input parameter for radiative transfer models as the orientation of leaves in canopy together with foliage density and sun angle influence how light is intercepted and interacts among leaf layers as it penetrates the plant canopy. Besides, it is important for photosynthesis estimation (Lemeur, 1973; Wit, 1965). The orientation of leaves also affect the reflectance observed by the satellite sensors (Knyazikhin et al., 2013; Verhoef & Bach, 2007).

The field measurement of LAD is tedious (De Wit, 1965). The existing methods are point quadrat method(Wilson, 1960), spatial coordinate apparatus developed by Lang (Lang, 1973; Shell, Lang, & Sale, 1974; W.-M. Wang, Li, & Su, 2007), and inclinometer/protractor (Hosoi, Nakabayashi, & Omasa, 2011; Pisek, Ryu, & Alikas, 2011; Stewart & Dwyer, 1999; Weligepolage, Gieske, & Su, 2012; Zou et al., 2014)in most cases. All these methods are time demanding (Zou et al., 2014). Efforts were also made using 3D data to study canopy structure, and the 3D data are either from laser scanning (Hosoi & Omasa, 2009; Omasa, Hosoi, & Konishi, 2007) or photogrammetry (Frasson & Krajewski, 2010). However, laser scanning is a resource demanding approach while photogrammetry requires professional knowledge and rigid operation. Recently, a digital photography (DP) method has been developed to measure LAD of tree species (Ryu et al., 2010) with simpler operation and more efficiency. The DP method has been verified to achieve a reliable result as manual measurement with inclinometer (Pisek et al., 2011). Zou et al., (2014) has adopted the DP method to study the canopy structure of field crops successfully.

LAD is complex in reality and difficult to largely sample in field, so it was initially assumed to be a consistent value in many calculations. However, it has been proved that this assumption introduces errors in photosynthesis estimation and other activities (Lemeur, 1973). Therefore, LIDF, mathematical description of LAD, were developed to approximate LAD of canopy. The most known and used ones are de Wit's four type canopy distribution, uniform distribution, spherical distribution, ellipsoidal distribution, rotated-ellipsoidal distribution, beta distribution and trigonometric function. The development of LIDF also contributes to fast development and improvement of LAI measurement instruments that are based on optical theory (Bréda, 2003).

1.2 Research problem

Canopy structure variables are so complicated to quantify in reality as it varies among/within species, cultivar, different growing stages as well as health status. Furthermore, it might also alter according to the surrounding environmental condition in order to survive or compete for more growing resource (Gustavo Angel Maddonni, Otegui, Andrieu, Chelle, & Casal, 2002). Various researches have been carried out on LAI or mean leaf angle (MTA) variation across growing season and among species, but few studies exist on the LAD variation. This study examines the LAD of maize canopy of different growing stage as well as different physiological maturity stage due to different environmental conditions.

As in reality LAD is so complex and difficult to measure, often assumptions of distribution are made that different LIDFs are developed to characterize LAD. Among all these mathematical expressions, spherical distribution is widely used because of its simplicity in computation (*i.e.* G-function remains constant regardless of viewing zenith angle). Ellipsoidal distribution is employed in canopy analyzing software CAN_EYE (M. Weiss & Baret, 2014) and commercial software LAI2000 (Weiss, 1991). However, assumptions often leads to inaccurate estimation of LAI (Lemeur, 1973; Liu et al., 2013; Pisek et al., 2011), as the LAD of different plant may not be necessarily subject to the assumed distribution. Some researchers find that 10% of the variation in LAI results from the effects of

alternative assumptions of LAD (Campbell, 1986; Thomas & Winner, 2000). In an effort to improve retrieval LAI, a close examination of LAD and its characterization closer to reality is therefore a key step.

Field manual measurement of LAD using inclinometer, protractor or other device mentioned above is tedious and time consuming. DP method was first applied by Ryu et al. (2010) , and has just become an interesting tool to measure plant canopy structure recently. It allows for fast and non-contact measurement of LAD, which shows great potential to overcome many shortcomings in other measurement techniques (Zou et al., 2014). The method has been validated on broadleaf trees (Pisek, Sonnentag, Richardson, & Mõttus, 2013) and several field crops (Zou et al., 2014). Maize, however, has totally different structure compared to those studies objects. Compared with broadleaf trees, maize has a much smaller canopy, and each individual leaf represents a bigger proportion of the whole canopy. Maize differs from the crops that have been studied by Zou et al. (2014) as it has a clear vertical profile, and the LAI and LAD vary in different vertical layer (Stewart & Dwyer, 1999; de Wit, 1965). In addition, no research has been carried out on the minimum sample size needed to characterize LAD of crop canopy such as maize. Therefore, there should be adjustment when applying DP method to maize study. Besides, whether DP method could yield reliable and reproducible LAD of maize canopy remains to be explored.

1.3 Research objectives

There are two overall objectives in this study:

Overall objective 1:

The first objective is to find out whether LAD of maize plant in different development stages and different growing environment varies, and then examine the performance of LIDFs to see which one gives the best fit and how it affect LAI using the gap fraction theory. The best LIDF will then be used to run the physical radiative transfer model to see the effect of different LAD on reflectance.

Overall objective 2:

Adjust DP based method and apply it on maize canopy measurement. Test and evaluate its usability for measuring maize canopy.

Specific objectives of 1:

1. Investigate LAD of maize plants in different development stages and different growing environment to see whether difference exists.
2. Fit LIDFs using manual measurement and find the LIDF that best characterizes maize canopy.
3. Examine the effect of using assumed LIDF on retrieving LAI based on the gap fraction theory at 57° viewing angle.
4. Investigate the influence of LAD on vegetation reflectance using a physical soil-leaf-canopy radiative transfer model.

Specific objectives of 2:

1. Apply DP methods to characterize maize LAD and compare with manual measurement.
2. Quantitatively assess the influence on projection function G, extinction coefficient K and LAI when LAD derived from DP method.
3. Find the minimum sample size to obtain a reasonable well and reproducible LAD.

1.4 Research questions

Research question 1:

Does the LAD of maize plants in this study significantly differ at different development stages?

Research question 2:

Is the LAD retrieved form DP method significantly different from that of manual measurement?

1.5 Hypothesis

1. Hypothesis 1

H0: The LAD of maize plants in this study significantly differs in different development stages.

H1: The LAD of maize plants in this study does not significantly differ in different development stages.

2. Hypothesis 2

H0: The LAD retrieved from DP method and manual measurement are not significantly different.

H1: The LAD retrieved from DP method and manual measurement are significantly different.

2. Material and methods

2.1 Theory

2.1.1 The gap fraction theory and LAI

Gap fraction is the probability that a light beam reaches ground without contacting the plant elements (Weiss, 2004), it is also used to measure light transmittance or penetration through canopies. Following Nilson (1971)'s study, the logarithm of the gap fraction is linearly related to downward accumulative foliage area index and this agrees well with experimental observations. There are three models to describe this relationship: the Poisson model, binominal model, markov model, among which the Poisson model are widely used due to its simplicity. Eq.2.1 is the expression of gap fraction $P_0(\theta,\phi)$ based on Poisson model in beam direction (θ,ϕ). It describes the penetration properties of light through canopies according to Beer lambert's law.

$$P_0(\theta,\phi) = \exp(-K(\theta,\phi)L) \tag{2.1}$$

Where L stands for effective LAI. The true LAI can be derived through averaging logarithm of gap fraction strategy (Lang and Xiang 1986, Demarez 2008, Liu 2013) which eliminates the clumping effects of leaf distribution.

2.1.2 Relations between gap fraction and leaf angle distribution

The effect of LAD on radiation attenuation can be described using projection function. Projection function G is the projected coefficient of unit leaf area on a plane perpendicular to the viewing direction (Nilson, 1971; Ross, 1981), and is related to LIDF $f(\theta_l)$ through eq.2.2 when assuming random distribution of leaf azimuth angles (Wilson, 1967).

$$G(\theta) = \int_0^{\pi/2} A(\theta,\theta_l)\, f(\theta_l) d\theta_l \tag{2.2}$$

$$A(\theta,\theta_l) = \cos\theta\cos\theta_l \ , \ if \left|\cot\theta\cot\theta_l\right| > 1 \tag{2.3}$$

$$A(\theta,\theta_l) = \cos\theta\cos\theta_l\left[1+\frac{\pi}{2}(\tan\psi-\psi)\right] \ , \ otherwise \tag{2.4}$$

$$\psi = \cos^{-1}(\cot\theta\cot\theta_l)$$

$$K(\theta,\phi) = \frac{G(\theta,\phi)}{\cos(\theta)} \tag{2.5}$$

Where θ is the viewing zenith angle. The relationship between projection function G and extinction coefficient K is denoted through eq. 2.5. It represents the average projection of unit leaf area on to a horizontal surface (Campbell, 1986). It can also be described as the mean number of interceptions in a leaf layer of unit leaf area along the penetration direction (Lemeur, 1973).

2.1.3 The leaf inclination distribution and its functions

As mentioned above, the calculation of projection function G requires knowledge of leaf inclination angle distribution functions. Several types of LIDF have been developed to characterize plant canopy, and they can be divided into three categories: (1) non-parametric function (de Wit, 1965) (2) one parameter function (Campbell, 1986; Thomas & Winner, 2000) (3) two-parameter function (Goel & Strebel, 1984; Verhoef, 1997).

According to Nichiporovich's (1961) measurement, quoted by de Wit (1965), the leaves of a canopy in general do not show a preferred azimuth direction. This was confirmed by de Wit's study, which also point out incorporating this orientation in the calculation is unrealistic (de Wit, 1965). Therefore only inclination angle is sufficient to characterize the position. Most LIDFs thus are simplified to only consider leaf inclination angle assuming that leaves are randomly distributed in azimuth direction.

(1) de Wit's LIDFs

de Wit (1965) classified canopy into four types according to their accumulative frequency of leaf angle occurrence (Figure 1). The mathematical expressions characterize the four type canopy (Table 1) were given by Verhoef and Bunnik (1975).

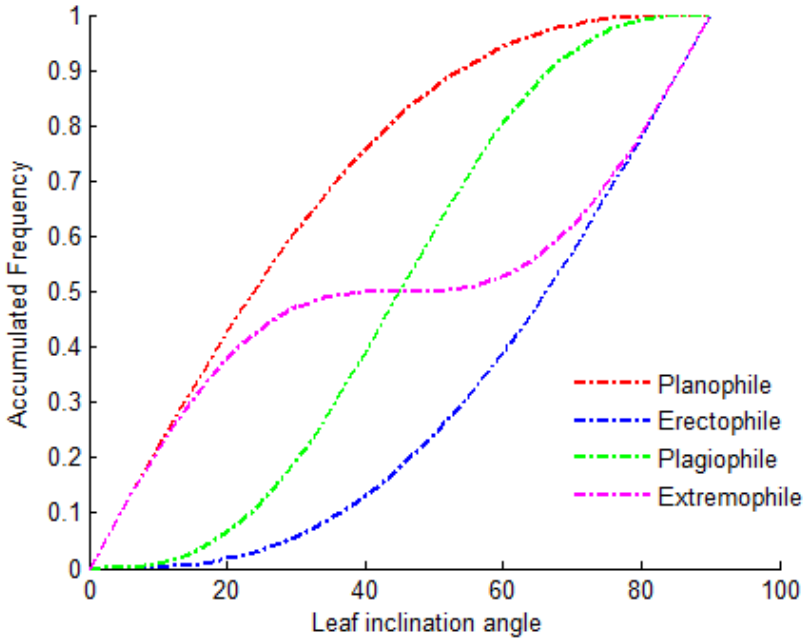

Figure 1 Accumulative frequency of four type canopy proposed by de Wit (1965)

Table 1 Four types of canopy and their LIDFs

Canopy type	Distribution function	Description
Planophile	$f(\theta_l)=\frac{2}{\pi}(1-\cos 2\theta_l)$	Horizontal leaves are most frequent
Erectophile	$f(\theta_l)=\frac{2}{\pi}(1+\cos 2\theta_l)$	Vertical leaves are most frequent
Plagiophile	$f(\theta_l)=\frac{2}{\pi}(1-\cos 4\theta_l)$	Oblique inclination are most frequent
Extremophile	$f(\theta_l)=\frac{2}{\pi}(1+\cos 4\theta_l)$	Oblique inclination are least frequent

Note: $f(\theta_l)$ is the leaf inclination angle distribution function; θ_l is the leaf inclination angle in radian.

(2) Spherical distribution

Spherical leaf angle distribution is a theoretical distribution (eq. 2.6). If sphere surface is considered made up of small unit elements, each element will have a normal. It is assumed that leaf inclination angles distribution is the same as that of the surface elements of a sphere (de Wit, 1965). Grasses, small grains and corn manifest spherical distribution according to Nichiporovich (1961). Spherical distribution assumption is widely used in physical models or instruments due to its simplicity and is parameter free (Pisek et al., 2013; Zou et al., 2014).

$$f(\theta_l)=\sin\theta_l \tag{2.6}$$

(3) Ellipsoidal leaf angle distribution

The spherical model, however, lacks flexibility (Campbell, 1986). By considering the distribution of surface area on a prolate or oblate spheroid rather than just spheroid, Campbell (1986) proposed the ellipsoidal model (eq. 2.7) which gives more realistic and flexible description of canopies. This model adjusts the ratio of horizontal to vertical axis of the spheroid using a parameter, so that LAD of any canopy structure (the four types in Table 1) could be simulated. It has been widely used to represent LAD by researchers (Bréda, 2003; Flerchinger & Yu, 2007; W.-M. Wang et al., 2007; Y. P. Wang & Jarvis, 1988; M. Weiss et al., 2004; Zheng & Moskal, 2012; Zou & Mõttus, 2015). The function is shown in eq.2.7:

$$f(\theta_l)=\frac{2\chi^3\sin\theta_l}{\Lambda(\cos^2\theta_l+\chi^2\sin^2\theta_l)^2} \tag{2.7}$$

When $\chi<1$,

$$\Lambda=\chi+(\sin^{-1}\varepsilon)/\varepsilon\ ,\quad \varepsilon=(1-\chi^2)^{1/2} \tag{2.8}$$

And when $\chi > 1$,

$$\Lambda = \chi + \frac{\ln[(1+\varepsilon)/(1-\varepsilon)]}{2\varepsilon\chi}, \quad \varepsilon = (1-\chi^{-2})^{1/2} \tag{2.9}$$

Where, χ stands for the ratio of horizontal semi-axis length to the vertical semi-axis length of an ellipsoid. θ_l is the leaf inclination angle. Eq. 2.10 relates χ to the mean leaf inclination angle $\overline{\theta_l}$ (in radius). To derive χ, eq. 2.11, as the inversion of eq.2.10, is used.

$$\overline{\theta_l} = 9.65(3+\chi)^{-1.65} \tag{2.10}$$

$$\chi = (\frac{\overline{\theta_l}}{9.65})^{-0.6061} - 3 \tag{2.11}$$

The mean leaf inclination angle is calculated using eq. 2.12 considering discrete leaf angle measurement (W.-M. Wang et al., 2007),

$$\overline{\theta_l} = \sum_{j=0}^{N} \theta_j F_j \tag{2.12}$$

Where F_j is the leaf area proportion for a leaf inclination angle interval which has a center value θ_j.

(4) Rotated-ellipsoid distribution

The rotated-ellipsoid distribution (eq. 2.13) was proposed by Thomas and Winner (2000) to handle the situation where high frequency of foliage angle at 0 occurs which is considered to be functional optimum for plants from ecological perspective (W.-M. Wang et al., 2007). As the ellipsoid function is constrained to give 0 values at inclination angle of 0°, it sometimes failed to represent canopies of such cases.

$$f(\theta_l) = \frac{2\chi^3 \cos\theta_l}{\Lambda(\sin^2\theta_l + \chi^2\cos^2\theta_l)^2} \tag{2.13}$$

The calculation of the parameters is the same as for ellipsoidal distribution, and they are paired mirror images for any giving χ. The parameter χ is obtained using eq.8 as well, but the mean leaf angle $\overline{\theta_l}$ is derived after transforming θ to $(\frac{\pi}{2} - \theta)$.

(5) Beta distribution

The two-parameter beta distribution proposed by Goel & Strebel (1984) not only represent well the ideal distribution of the four types of canopy but also agree with field measurement

of LAD. The study done by Wang et al. (2007) also points to the same direction that beta distribution fits reasonably well the natural vegetation LAD and better than the other distribution models mentioned above. Recently, the beta distribution has been applied in several studies on measuring LAD using photographic methods (Pisek et al., 2011; Zou et al., 2014). Eq. 2.14 is the beta distribution function:

$$f(t) = \frac{1}{B(\mu,\nu)}(1-t)^{\mu-1}t^{\upsilon-1} \tag{2.14}$$

Where $B(\mu,\nu)$ is the Beta distribution (Gupta & Nadarajah, 2004) defined as eq. 2.15 below; $t = 2\theta_l / \pi$ and θ_l is the leaf inclination angle in radians.

$$B(\mu,\nu) = \int_0^1 (1-x)^{\mu-1}x^{\upsilon-1}dx = \frac{\Gamma(\mu)\Gamma(\nu)}{\Gamma(\mu+\nu)} \tag{2.15}$$

Where Γ is Gamma function. Parameter μ and ν are two parameters related to $\bar{t}$, and determined by eq. 2.16 and eq.2.17:

$$\mu = (1-\bar{t})(\frac{\sigma_0^2}{\sigma_t^2}-1) \tag{2.16}$$

$$\nu = \bar{t}(\frac{\sigma_0^2}{\sigma_t^2}-1) \tag{2.17}$$

Where σ_0^2 and σ_t^2 are the maximum variance and variance of t respectively, and calculated using eq. 2.18:

$$\begin{aligned} \sigma_0^2 &= \bar{t}(1-\bar{t}) \\ \sigma_t^2 &= \mathrm{var}(t) \end{aligned} \tag{2.18}$$

(6) Trigonometric function

Trigonometric function (eq. 2.19) was proposed by Verhoef (1997) to model the leaf angle distribution which is one of the important canopy architecture parameters for physical process based radiative transfer model SAIL. This method can be regarded as a "graphic" method, which first takes the accumulative frequency of uniform distribution as a basis, then rotates the coordinate system by using the diagonal as X axis of trigonometric function, and the direction perpendicular to the diagonal Y axis (Verhoef, 1997) as shown by Figure 2. The parameter *a* controls the mean leaf inclination angle while *b* affects the bimodality. By using different combination of the two parameters, *a* and *b* , *a* variety of canopy type can be modelled including the four type classified by de Wit (1965). The function is constrained by eq. 2.21 to ensure the accumulative frequency is monotonously increasing.

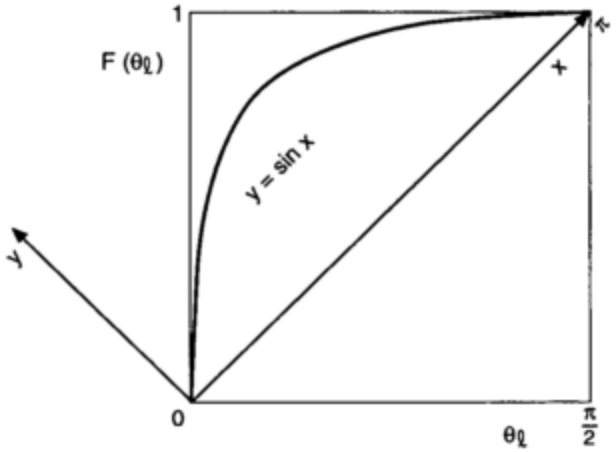

Figure 2 Demonstration of graphical method of trigonometric function and coordination transformation (Verhoef, 1997).

$$y = a\sin x + \frac{b\sin 2x}{2} \tag{2.19}$$

$$\begin{aligned} x &= \frac{\pi}{2}F(\theta_l) + \theta_l \\ y &= \frac{\pi}{2}F(\theta_l) - \theta_l \end{aligned} \tag{2.20}$$

$$|a| + |b| \le 1 \tag{2.21}$$

x and y are related to the accumulative frequency $F(\theta_l)$ of leaf inclination angles through eq. 2.20, which can be obtained through a giving distribution. The range of x is from 0 to π. Through inverse of eq. 2.20, the accumulative distribution can be obtained through eq.2.22.

$$\begin{aligned} \theta_l &= \frac{(x-y)}{2} \\ F(\theta_l) &= \frac{(x+y)}{\pi} \end{aligned} \tag{2.22}$$

The best fitting parameters a and b are obtained through least square fitting of a given LAD. This was done in the x-y domain by minimizing the sum of squared residues in y values (Verhoef, 1997; W.-M. Wang et al., 2007). However, a more robust and better fit can be achieved through fitting in the original $F(\theta_l)$ and θ_l domain, which means $C = \sum (F(\theta_l) - F'(\theta_l))^2$ has to be minimized, where $F(\theta_l)$ is the observed accumulative frequency and $F'(\theta_l)$ is the fitted one at the angle θ_l. The cost function C can also be written as eq. 2.23 or eq. 2.24:

$$C = \sum (F(\theta_l) - \frac{x+y}{\pi})^2 \tag{2.23}$$

or

$$\pi^2 C = \sum (\pi F(\theta_l) - (x+y))^2 = \pi^2 \sum F(\theta_l)^2 - 2\pi \sum F(\theta_l) x + \sum x^2 - 2\pi \sum F(\theta_l) y + 2\sum xy + \sum y^2 \tag{2.24}$$

The last three items will be minimized since they only depend on a and b, which can be further expressed as eq. 2.25 if y is substituted using eq. 2.19:

$$\begin{aligned} B = &\sum (a^2 \sin^2 x + ab \sin x \sin 2x + \frac{1}{4} b^2 \sin^2 2x) + \\ &2\sum xa \sin x + 2\sum x \frac{1}{2} b \sin 2x - 2\pi \sum F(\theta_l)(a \sin x + \frac{1}{2} b \sin 2x) \end{aligned} \tag{2.25}$$

To minimize B, the partial derivatives with respect to a and b should be zero as eq. 2.26 shows:

$$\begin{aligned} \frac{\partial B}{\partial a} &= 2a \sum \sin^2 x + b \sum \sin x \sin 2x + 2\sum x \sin x - 2\pi \sum F(\theta_l) \sin x = 0 \\ \frac{\partial B}{\partial b} &= a \sum \sin x \sin 2x + \tfrac{1}{2} b \sum \sin^2 2x + \sum x \sin 2x - \pi \sum F(\theta_l) \sin 2x = 0 \end{aligned} \tag{2.26}$$

Parameter a and b are the solution of matrix equation eq. 2.27:

$$\begin{pmatrix} \sum \sin^2 x & \frac{1}{2}\sum \sin x \sin 2x \\ \sum \sin x \sin 2x & \frac{1}{2}\sum \sin^2 2x \end{pmatrix} \begin{pmatrix} a \\ b \end{pmatrix} = \begin{pmatrix} \pi \sum F(\theta_l) \sin x - \sum x \sin x \\ \pi \sum F(\theta_l) \sin 2x - \sum x \sin 2x \end{pmatrix} \tag{2.27}$$

2.2.3 57.5° theory

Although the projection function G depends on LIDF, it was found that G almost remains a constant about 0.5 when viewing at a zenith angle of 1 radius (57.5°) (Warren-Wilson, 1963). Bonhomme et al (Bonhomme, Grancher, & Chartier, 1974) applied the technique to estimate LAI of crops and found good agreement with the actual LAI values. When G functions remains 0.5 at this viewing angle, K will be 0.93 correspondingly. LAI could be easily obtained through calculating eq. 2.28:

$$L = \frac{-\ln(P_o(57.5^\circ))}{0.93} \tag{2.28}$$

Where $P_o(57.5^\circ)$ is the gap fraction at 57.5° viewing zenith angle. This method has been a research interest (Confalonieri et al., 2013; Liu et al., 2013; M. Weiss & Baret, 2014) as it proves a simple and fast way to quantify LAI. The LAI in this study refers to effective LAI which does not take into account clumping effect.

2.2 Data collection

2.2.1 Study Site

The field measurement was conducted in a maize field from a farm in Rossum, Netherlands (52 22` 18.6``, 6 57` 54.55``, 17 m above sea level) from the 8th of October to 31st October, 2014. The size of the maize field is about 200 m long and 50 m wide (ca. 1 hectare), and it was heterogeneous field where large variation in terms of environmental conditions, and crop height, maturity stages were found (Figure 26 in Appendix).

According to the interview with the farmer, all maize crops were planted at the same period around 15th-20th of June, 2014. The majority of the maize was at late reproductive stage and close to physiological maturity stage. In the corner of the field, some short plants which were about 50 cm tall were still in vegetative stage. The big variation in height was caused by two factors: (1) the different soil type in the field; (2) different level of suffering from water logging (Figure 27 in Appendix). There are two types of soil in different part of the field, loam soil and black soil. The black soil is rich in nutrition and do not have much water logging effect. The maize plants that were found in black soil area and not affected by the water logging were tallest in the field, up to 2.7m or even higher. Those planted in loam soil and severely suffered from water logging were found shortest, only up to 50 cm. In transition area in terms of water logging condition and soil type, medium height maize plants were seen (Figure 3). A stratified random sampling strategy thus was applied. As it was approaching the end of the maize growing season, the majority of plants had 7 to 10 healthy leaves left. The very bottom leaves were either dead or broken off.

2.2.2 Sampling method

The maize field was visually divided into 5 categories according to the height. In the field close to category 3, the maize plants looked different from the rest since all leaves of appeared to be almost horizontal. They were also sampled and were named category 6 (Table 2). Within each category, random sampling was applied. The row and column of sampled crop were generated by an online random generator. If the random selected plants had broken leaves or was already dry, its neighboring plant with healthy leaves was sampled.

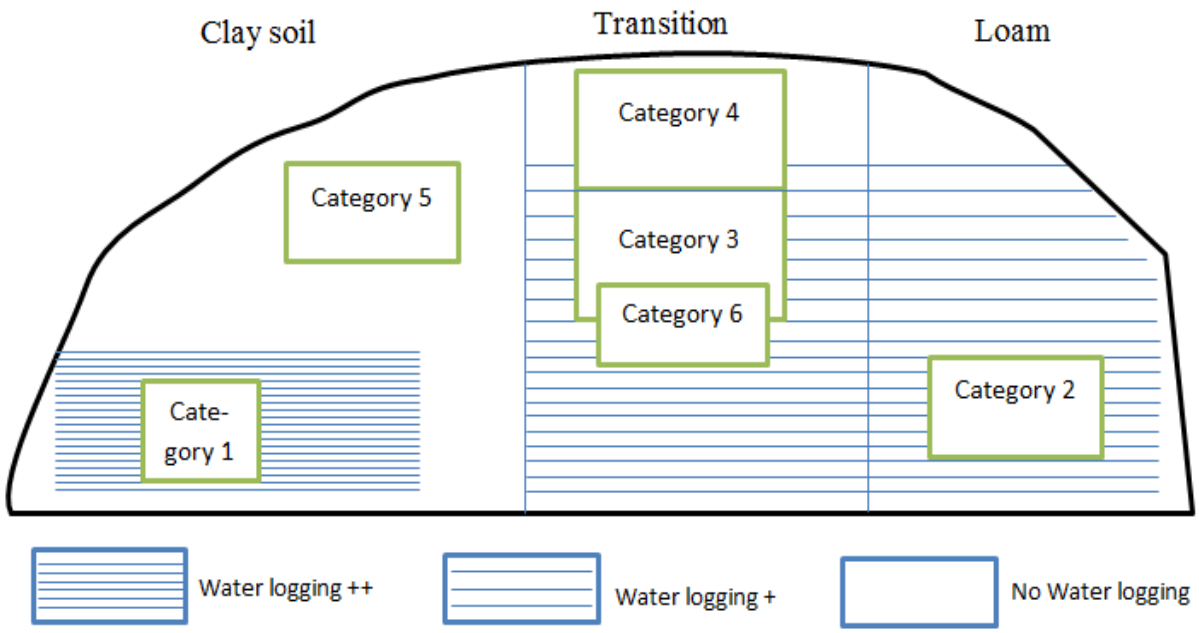

Figure 3 Environmental condition of sampled field

Table 2 Description of field sample data

Categories	Height (m)	Size (m × m)	Sampled plants	Sampled leaves	Sampled angles
Category 1	Ca. 0.3- 0.6	5×5	15	108	269
Category 2	Ca. 0.8- 1.5	40×10	22	164	487
Category 3	Ca. 1.5- 2.0	40×15	19	139	446
Category 4	Ca. 2.0	30×15	20	162	518
Category 5	Ca. 2.3-2.7	30×10	15	130	445
Category 6	Ca. 0.8-1.5	12×8	15	81	201

2.2.3 Manual measurement of leaf angle

Leaf inclination angle is defined as the angle between the zenith direction and the normal of the leaf surface. Most studies use inclinometer to measure leaf angles, which is direct measurement and is widely used as a way to obtain reference values of leaf angles(Hosoi & Omasa, 2009; Pisek et al., 2011). In this study, a portable digital angle ruler (Machine DRO) was used instead of an inclinometer. The ruler is 200mm long, and has a resolution of 0.1° and accuracy of 0.3°. Each leaf of the sample plant was measured. For leaves that are flat, only one angle was measured. For leaves that bent due to its length and weight, one single angle could not represent the inclination of the whole leaf, thus the leaves were visually divided into several leaf segments which could be regarded as flat plane, and then inclination angle of each leaf segment was measured. Total leaf area and leaf length were measured using LI-3000C portable leaf area meter (Li-COR, Lincoln, NE). The leaf segment area was calculated by multiplying its corresponding proportion with the total leaf area. Leaf area of

each measured angle was counted and later served as input to obtain leaf angle distribution. The whole measurement was done under calm condition to avoid wind effects on leaves.

2.2.4 Adjusted digital photographic measurements of leaf angle

Panosonic DMC FH2 camera with a resolution of 14mega pixel was used to perform DP measurements. A water bubble level was stuck to the side of the camera to ensure the photo was taken leveled. The camera was about 1m away (Zou et al., 2014) from the leaves when taking photos and was held leveled. No zooming was performed during the entire field measurement. In previous studies on trees or crops, the photos were taken at individual plant level (Zou et al., 2014) or different vertical position of a tree canopy (Pisek et al., 2011; Ryu et al., 2010). The method, however, was adjusted to best characterize maize canopy in this study by taking photos of each individual leaf of a sampled plant. The photos were always taken perpendicular to the leaves as much as possible to ensure that measured inclination angles on the photo are correct and valid. Only categories 1-4 and category 6 were measured, as for category 5 (the tallest maize) leaves were easily broken during the measurements because of high planting density. In order to protect the crop, DP measurement was not conducted for this category. The angle measurement was performed using angle tool of the open source image processing software ImageJ[1], which was used in the previous leaf angle distribution studies on forest trees (Pisek et al., 2011; Ryu et al., 2010) and field crops (Zou et al., 2014). Same as the manual measurement, for flat leaves in the upper layer, only one angle was measured, while for the rest curved leaves, angles of leaf segments were measured (Figure 4).

Figure 4 Demonstration of angle measurement on digital photograph

Leaf area represented by each inclination angle is needed to calculate LAD; however, it is impossible to measure the leaf area in the photo. To address this problem, an area function depending on relative length was proposed and was derived through two steps, width function establishment and area calculation. It is possible to measure relative length of each leaf

[1] http://rsbweb.nih.gov/ij/

segment on the photo, and this measured quantity is not as much affected by distance variation between the camera and the plant as the other metrics such as absolute length as long as the camera view is perpendicular to the leaf. The area can be obtained through integration of the leaf width along the length direction at a very small step.

(1) Width function

It is not possible to measure the leaf width on the photo either, thus the width has to be modeled as a function of relative length first. The leaf was divided into 10 segments of equal length, and each segment length has a relative length of 0.1 (Figure 5). A polynomial was employed to model the width at each relative length position.

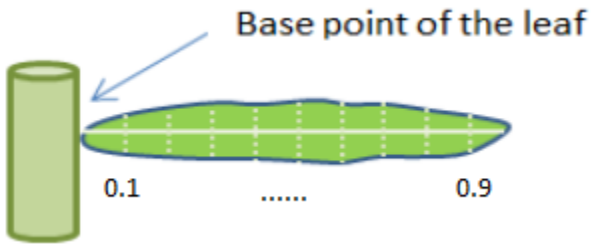

Figure 5 Demonstration of relative length of maize leaf

Each category has a width function because the leaf size and shape are different among the groups according to field observation. Within the category, the leaves have more or less similar shape, thus a base function characterizing the leaf shape of the category were first generated. By multiply the shape factor of each individual leaf, the complete width function was obtained. For each category, around 20 - 40 numbers of leaves were measured. The width at the 10 relative length positions of each leaf, the total leaf length and leaf area were measured (Table 3).

Table 3 Leaf sample size of each category

Group	Category 1	Category 2	Category 3	Category 4	Category 6
Leaf sample	22	31	37	39	33

The base function was fitted using a 3rd order polynomial (eq. 2.29). Zou et al. (2014) used a 4^{th} order polynomial of relative length to estimate the leaf width of cereal crops (wheat, barley and oat). In this study, it was found that 3^{rd} order is powerful enough to approximate the width. Considering the model efficiency, 3^{rd} order is faster and less complex, thus were applied here. A shape factor α (eq. 2.30) was then used to adjust the width resulting from base function to best fit the shape of each individual leaf in the category. In the study of Stewart and Dwyer (1993) and Mauro (Homem Antunes, Walter-Shea, & Mesarch, 2001), two shape parameters were used. However, the parameters themselves are empirical ones and not related to the leaf property, and the way to derive the parameters is also labor intensive. The shape factor used in

this study is associated with the leaf area and the overall leaf shape properties of the category (eq. 2.31).

$$w_{base} = p_0 + p_1 * l + p_2 * l^2 + p_3 * l^3 \tag{2.29}$$

$$w_{adjust} = w_{base} * \alpha \tag{2.30}$$

$$\alpha = c_{category} \frac{s^{12/5}}{\max w_{base}} \tag{2.31}$$

Where w_{base} is width calculated by the polynomial, l is the relative length, p_0, p_1, p_2 and p_3 are the coefficients, α is the leaf-specific shape factor, w_{adjust} is the adjusted width, s is total area, $\max w_{base}$ is the maximum width from the polynomial fitting of each leaf, and $c_{category}$ is a category specific parameter.

To determine parameter $c_{category}$, a bootstrap technique was used. The initial range of $c_{category}$ was given in Table 4. $c_{category}$ was modified each time at a step of 0.01. The value that yields the minimum RMSE in validation for each category was recorded.

Table 4 Initial value range of $c_{category}$ for different categories

Group	Category 1	Category 2	Category 3	Category 4	Category 6
$c_{category}$ range	0.58-0.68	0.72-0.82	0.64-0.74	0.64-0.74	0.62-0.68

Considering the relatively small sample size, the boot strap technique was applied in such a way that the whole sampled data was randomly divided to training (2/3) and validation (1/3) sets respectively to form 300 data sets. The model has been run 300 times using these datasets, and then the average of the recorded $c_{category}$ value for each category was chosen to be the optimal parameters.

The shape factor α then can be calculated once the $c_{category}$ is known. The polynomial coefficients p_0, p_1, p_2 and p_3 were obtained using linear least square estimation. The bootstrap technique was also used here to get robust results. The average values of each running results were treated as the optimal coefficients.

(2) Area calculation

Area function depends on both the width function and relative length. It is the sum of the leaf increment area eq. 2.32.

$$s = \sum s_i \tag{2.32}$$

Leaf increment area s_i is the integration of width along the leaf tip direction at a small step as eq. 2.33 (Stewart & Dwyer, 1993).

$$s_i = \int_{l_{i-1}}^{l_i} wdl \tag{2.33}$$

In this study, the leaf increment area was treated as trapezoid, thus the lead segment area calculation was using eq. 2.34:

$$s_i = \frac{(w_{i-1} + w_i)\, d_i}{2} L \tag{2.34}$$

Where d_i is the distance between the width at relative length l_{i-1} and l_i. L is the total length of the leaf.

The inclination angles of the leaf segment as well as the relative length of the leaf segment were measured on the photo, and then the leaf area associated with the leaf angle was calculated using eq. 2.29 and eq. 2.34.

2.2.4 Digital photograph measurement of gap fraction

Gap fraction was measured in category 2 using a digital photography method. A Canon EOS Mark II 5D camera with a normal lens was used to take photos of maize canopy. The camera and a digital inclinometer (Wixey, WR300-KIT) was installed on a platform and mounted on a tripod. The platform was raised to 1m above the maize canopy as recommended in previous study (Demarez, Duthoit, Baret, Weiss, & Dedieu, 2008). The camera was set to have a normal exposure and 35mm focal length. Starting from the camera looking downwards (15°-20° bias from strictly downwards) to the maize canopy, the inclinometer was turned on to record the inclination angle of the platform thus the viewing angle of the camera could be known. A video was taken as the platform was rotated to certain angles. These operations have been repeated at every sample point. Later the photo frames that were taken at viewing angle 50° to 59° with 1° step were picked out from the video stream and put into CANEYE software (M. Weiss & Baret, 2014) for further processing. Gap fraction at these viewing angles was obtained. A systematic point sampling method was employed here, and in total 50 plots of 6×4 m^2 size was measured.

2.3 Data processing and analysis

2.3.1 LAD

The measured inclination angles from both manual measurement and DP method were grouped into bins from 0 ° - 90 ° with an interval of 5 °. The center angle of each bin was

reported, and the leaf area of leaf segments located in each angle bin were divided by the total leaf area summed from all bins to obtain the frequency LAD (Table 17 and 18 in appendix). The azimuth angles of the maize crop were assumed to be uniformly distributed in this study following the other studies (Pisek et al., 2011, 2013; Zou et al., 2014). For LAD of each category, the deviation from the classical canopy types was quantified using a modified incliantion index eq. 2.35 (Pisek et al., 2013) which was first proposed by Ross (1981).

$$x_L = \int_0^{\pi/2} \left| f(\theta_L) - f_{classic}(\theta_L) \right| d\theta_L \tag{2.35}$$

Where $f_{classic}(\theta_L)$ represent the four canopy type given by de Wit (1965) and quantified by Verhoef & Bunnik (1975).

Besides, to further understand the LAD through canopy layers, all sampled leaves were pooled together and divided into groups according to their position on the stem. The top leaf is flagged as number 1, the second as number 2, till the very bottom as number 10. Then LAD of each layer was calculated and compared.

2.3.2 LIDF

The manual measurements were used to fit LIDFs. Eq.2.7 and eq. 2.13 were employed to determine the one parameter LIDFs ellipsoidal distribution and rotated-ellipsoidal distribution, and eq.2.14 and eq. 2.19 for the two-parameter LIDFs beta distribution and trigonometric function. The parameters of these LIDFs were retrieved using the fitted result to ensure the fitting was correct, and were compared with the values from the previous studies on other plants. Root mean square error (RMSE) was used to quantitatively assess the performance of each LIDF.

Projection function G and extinction coefficient K were calculated using different LIDFs and compared. In turn LAI of category 2 was derived using the inversion of gap fraction model.

2.3.3 Statistical test

To answer the research question 1 and 2, a two sample Anderson-Darling test (A-D test) (Trujillo-Ortiz, Hernandez-Walls, Barba-Rojo, Cupul-Magana, & Zavala-Garcia, 2007) was used to test the hypothesis. In previous studies on LAD, Chi-square test, G test were also applied to examine the goodness of fit (Thomas & Winner, 2000; W.-M. Wang et al., 2007). However, both tests require equal sample size, which cannot be fullfilled in this study because the sample size which was determined by leaf area differs among categories. Therefore, A-D test were used. A-D test was a modified version of Kolmogorov-Smirnov test, which puts more weight on the tails of the test (Scholz & Stephens, 1987). A-D test was applied after consulting Jan Pisek, who has used both A-D test and K-S test in her studies on tree species (Pisek et al., 2011, 2013) and later found out that A-D test are more suitable for this type of study.

2.3.4 Minimum sample size

The leaf number available for LAD analysis varied between categories as plants have different numbers of leaves. The effect of different sample size (leaf number) on LAD was studied by comparing LAD resulted from sub dataset and the original dataset in each category to determine the minimum sample size. In each category, 100 sub datasets were generated by randomly selecting plants from original datasets for each sample size by using a bootstrapping technique. The sample size was from 4 up to 15 plants for categories 1 and 6, to 17 plants for categories 2 and 3 with a step of one plant each time. The agreement between the LAD results from sub dataset and original dataset was evaluated by the A-D test.

2.4 Reflectance simulation using SLC model

A soil-leaf-canopy physical model SLC was used to study the effect of different LAD on plant canopy reflectance. The model is chosen as it incorporates much media through which the light radiation passes(Rex, 2010). The model coupled modified Hapke soil BRDF model, PROSPECT leaf model, and 4SAIL2 canopy model as well as an atmospheric correction model to generate more realistic vegetation canopy reflectance (Verhoef & Bach, 2007).

To examine the effect of different canopy type on reflectance, different viewing angles, solar zenith angles and different LAI level were used. The parameter settings are shown in Table 5 and 6 respectively. The LIDF parameter *u* and *v* are other forms of trigonometric function parameters *a* and *b* (eq. 2.36-2.37), and work in pairs in this study instead of random combination. The values are derived through calculation using *a* and *b* result from the fitted trigonometric function of the 6 categories (seen in section 2.1.3). For example, -0.3708 and 0.5780 are for category 1 and are paired to run the model. The solar angle and relative azimuth angle were adjusted to best approximate the condition in the Netherlands. The other canopy architecture parameters were set based on previous study done on the vegetation (Verhoef & Bach, 2007). The calculated reflectance was composed of 80% bi-directional reflectance (sun radiation) and 20% hemispherical reflectance (diffuse radiation).

$$u = a + b \tag{2.36}$$

$$v = a - b \tag{2.37}$$

Table 5 The parameter setting to examine the effect of different viewing zenith angles (The result plot only shows reflectance at viewing angle between 0° to 30° to approximate the reality in the Netherlands)

Code	Parameter	values
Soil moisture	Soil moisture	0.05
Cab_green	CHL content(green leaves)	60
Cw_green	Water content(green leaves)	0.005
Cdm_green	Dry matter content (green leaves)	0.003
Cs_green	Senescence (green leaves)	0.03
N_green	Structure (green leaves)	1.5

Cab_brown	CHL content(brown leaves)	5
Cw_brown	Water content(brown leaves)	0.0025
Cdm_brown	Dry matter content (brown leaves)	0.01
Cs_brown	Senescence (brown leaves)	0.6
N_brown	Structure (brown leaves)	2
LAI	Leaf area index	1 2 4
LIDFu	Average leaf slope	-0.3708 -0.3154 -0.4465 -0.4772 -0.4090 0.1416
LIDFv	Leaf inclination angle distribution function bimodality	0.5780 0.6009 0.5642 0.4030 0.2052 0.9478
hot	Hot spot parameter	0.05
fB	Fraction of brown leaves	0
Diss	Canopy dissociation factor	0
Cv	Crown clumping	1
zeta	Crown cover	0.2
tts	Solar zenith angle	40
tto	View zenith angle	0 5 10 15 20 25 26 27 28 29 30 35 40 45 50 55 60 65 70 75 80 85 90
psi	Relative azimuth angle	45 135

Table 6 The parameter setting to examine the effect of different sun angles

Code	**Parameter**	**values**
Soil moisture	Soil moisture	0.05
Cab_green	CHL content(green leaves)	60
Cw_green	Water content(green leaves)	0.005
Cdm_green	Dry matter content (green leaves)	0.003
Cs_green	Senescence (green leaves)	0.03
N_green	Structure (green leaves)	1.5
Cab_brown	CHL content(brown leaves)	5
Cw_brown	Water content(brown leaves)	0.0025
Cdm_brown	Dry matter content (brown leaves)	0.01
Cs_brown	Senescence (brown leaves)	0.6
N_brown	Structure (brown leaves)	2
LAI	Leaf area index	1 2 4
LIDFu	Average leaf slope	0.3708 -0.3154 -0.4465 -0.4772 -0.4090 0.1416
LIDFv	Leaf inclination angle distribution function bimodality	0.5780 0.6009 0.5642 0.4030 0.2052 0.9478
hot	Hot spot parameter	0.05
fB	Fraction of brown leaves	0
Diss	Canopy dissociation factor	0
Cv	Crown clumping	1
zeta	Crown cover	0.2
tts	Solar zenith angle	30 35 40 45 50 55 60 65 70
tto	View zenith angle	0
psi	Relative azimuth angle	45 135

3. Results

3.1 Different physiological maturity stage

According to Table 7, the inclination index suggests categories 1-5 are subject to plagiophile type and category 6 are planophile type. The plagiophile categories have mean leaf angle from around 40° to 50°. The 6th category, majority of leaves were horizontal according to field observation, has a mean of 25° and are quantitatively characterized planophile type as expected. The accumulative frequency plot (Figure 6) points to the same direction. The mean and standard deviation statistics of planophile and plagiophile are also coincident with the findings by previous studies on tree species (Pisek et al., 2011; W.-M. Wang et al., 2007). It is worth mentioning that uniform and spherical distribution, which are often assumed in many cases (Goudriaan, 1988; Pisek et al., 2013) are the second and third most close canopy type as indicated by the inclination index. As the plant height increases in categories 2-5, the mean leaf angle rises 2°-3° correspondently, and the canopy LAD gets closer to spherical distribution as suggested by the inclination index.

The maize canopy is more or less spherical distribution according to Nichiporovich (1961), however, later on de Wit (1965) and Lemeur (1973) found that plagiophile canopy in maize were observed. This study partly confirmed their founding, because besides plagiophile, planophile canopy type also occurs.

Table 7 Statistics and inclination index of manual measurement of 6 categories

	Mean	Standard Deviation	Inclination Index					
			planophile	erectophile	plagiophile	extremophile	uniform	spherical
Category 1	41.10	17.48	0.73	0.94	**0.28**	1.22	0.59	0.71
Category 2	39.88	18.20	0.69	1.04	**0.37**	1.16	0.56	0.81
Category 3	42.77	16.89	0.79	0.97	**0.36**	1.30	0.69	0.77
Category 4	46.05	18.03	0.88	0.85	**0.45**	1.24	0.67	0.68
Category 5	48.23	20.13	0.94	0.61	**0.44**	1.03	0.53	0.48
Category 6	25.19	14.88	**0.36**	1.46	0.92	1.06	0.85	1.23

Both category 1 and category 6 significantly differ from the other categories (implied by the p values in Table 8). The differences among the rest categories 2-5, however, are not significant (P=0.07-0.61). This means that the maize plants in categories 2-5 have similar leaf angle distribution even though they have different height and grow in different environmental conditions (section 2.2.1). Maize in category 6 differs from the other categories visually since most leaves are horizontal. As expected, all tests reject the null hypothesis about the category 6 and the rest categories and suggest the significant difference exists.

Table 8 A-D test result of comparing the LAD of 6 categories

	category 1	category 2		category 3		category 4		category 5		category 6	
		D	P	D	P	D	P	D	P	D	P
category 1		11.3275	0.0000	6.8464	0.0001	10.2082	0.0000	11.5853	0.0000	2.7118	0.0344
category 2				0.6105	0.5667	1.0601	0.3204	1.6196	0.1446	6.3918	0.0003
category 3						1.1325	0.2894	2.0864	0.0767	4.3921	0.0044
category 4								0.5250	0.6193	6.9491	0.0000
category 5										8.9946	0.0000
category 6											

(Note: D is the A-D rank statistic, and P is the probability associated to the A-D rank statistic. The confidence level is set to be 95%. When P value is larger than 0.05, the null hypothesis is accepted.)

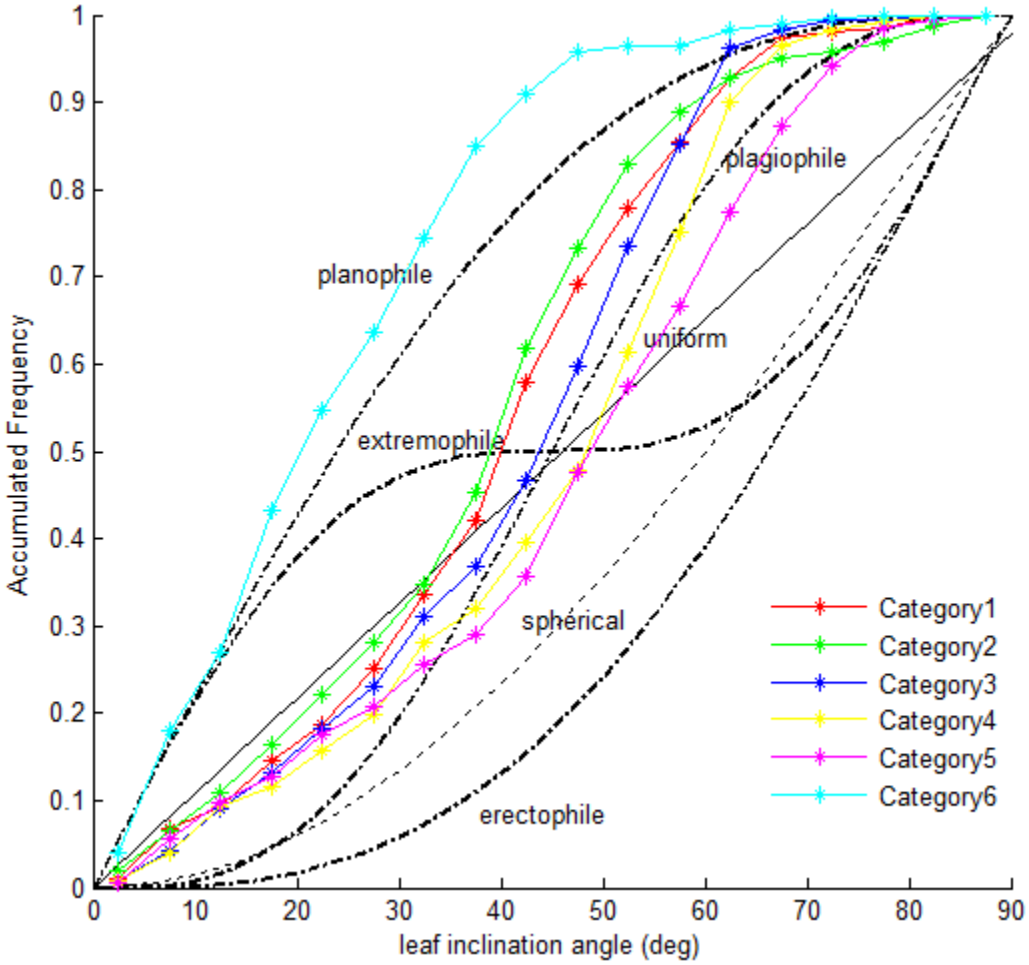

Figure 6 The accumulative frequency of measured LAD and LIDFs

3.2 Vertical profile

According to Figure 7, as going deeper through the canopy layer, mean leaf inclination angle decreases and levels out around 36°. The accumulative frequency plot (Figure 8) suggests the upper leaves are subject to plagiophile (purple line) and it gradually transits towards planophile (cyan line) types as going deeper through maize canopy. The LAD (Figure 9) of top leaves shows outstanding sharp peaks at leaf angle 60° while the middle leaves have the most frequently occurred leaf angles across a range from 40° to 60° rather than an single angle. This is because majority of top leaves (leaf 1-3) are flat leaves which just have one inclination angle, whereas the rest leaves are curved resulting in multiple inclination angles. This is further illustrated by the bottom LAD behavior (leaf 8, 9 and 10). The frequencies illustrate that multiple angles rather than just one angle occur frequently and the angles are between 10° and 60°, which means that LAD of bottom layer leaves are more uniformly distributed.

Agreement is found in comparison with Lemeur's work for upper layers as he reported high density for leaf angle above 65° in upper layers. A small density of 0°-20° was also reported for upper layers in his work; however, this is not seen in this study. Another difference between the two studies is that for lower leaves, extremely plagiophile is observed in his work while the accumulative frequency (Figure 8) in this study suggests somewhere in between plagiophile and planophile.

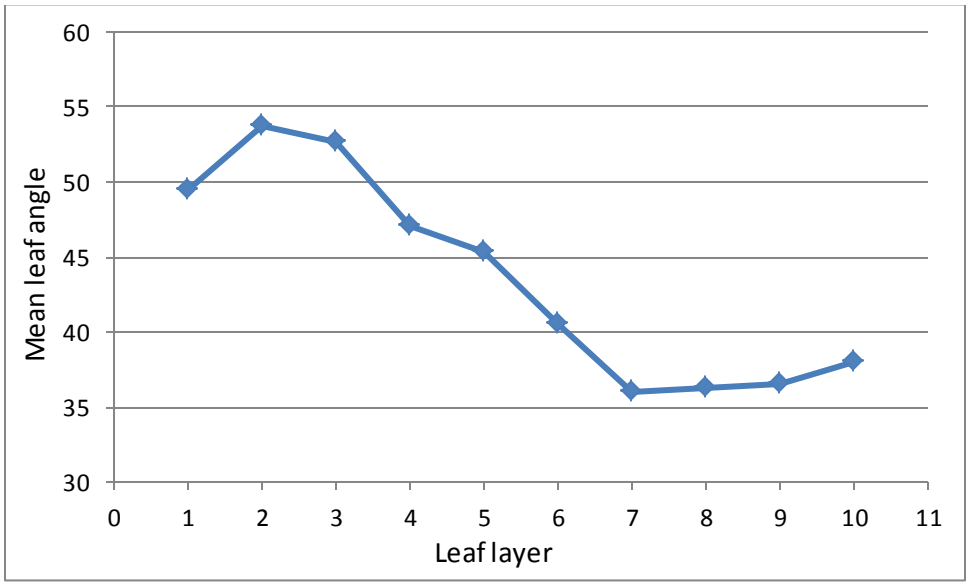

Figure 7 Mean leaf angle of each leaf layer

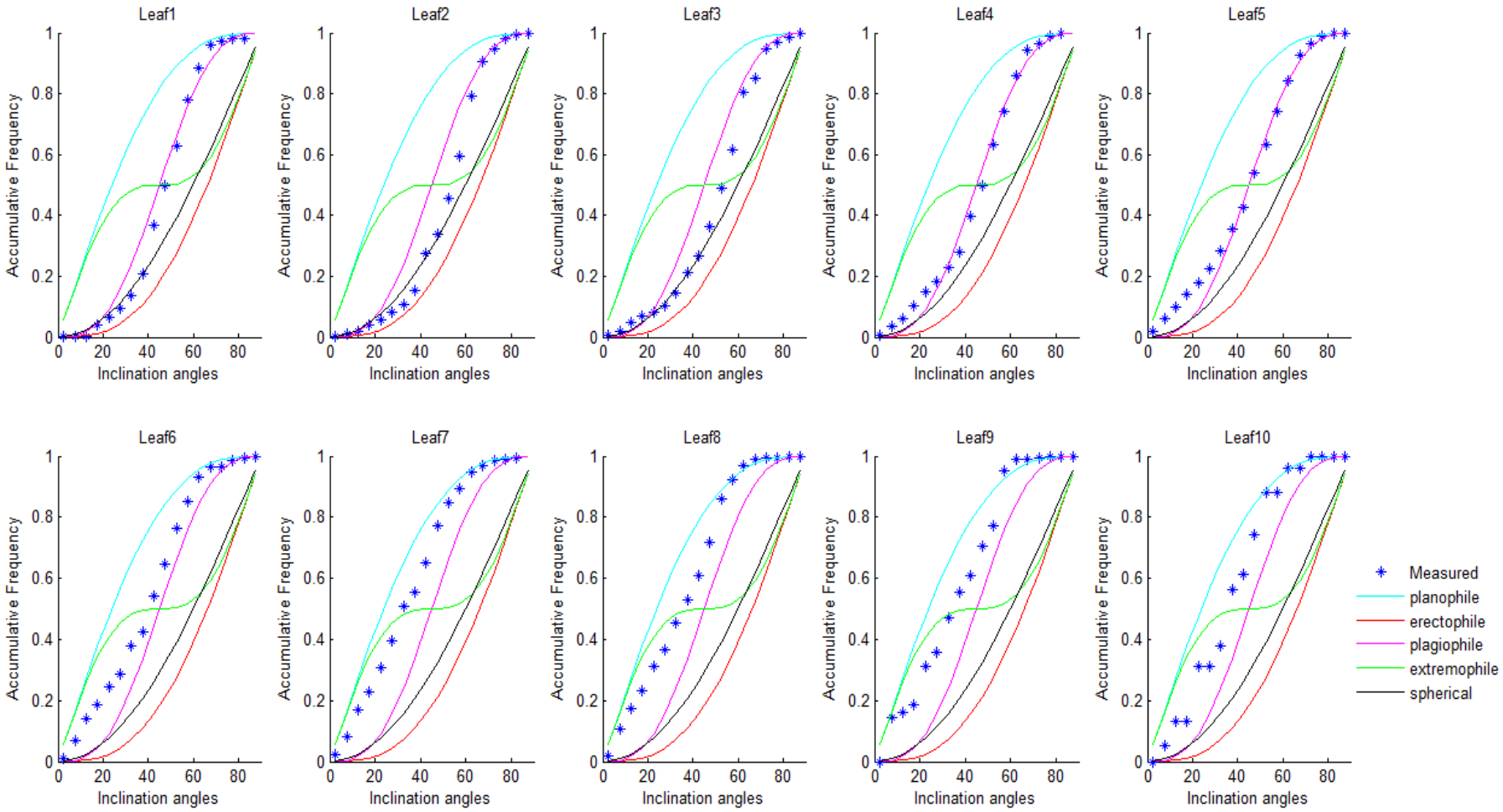

Figure 8 Accumulative frequency of LAD through vertical profile

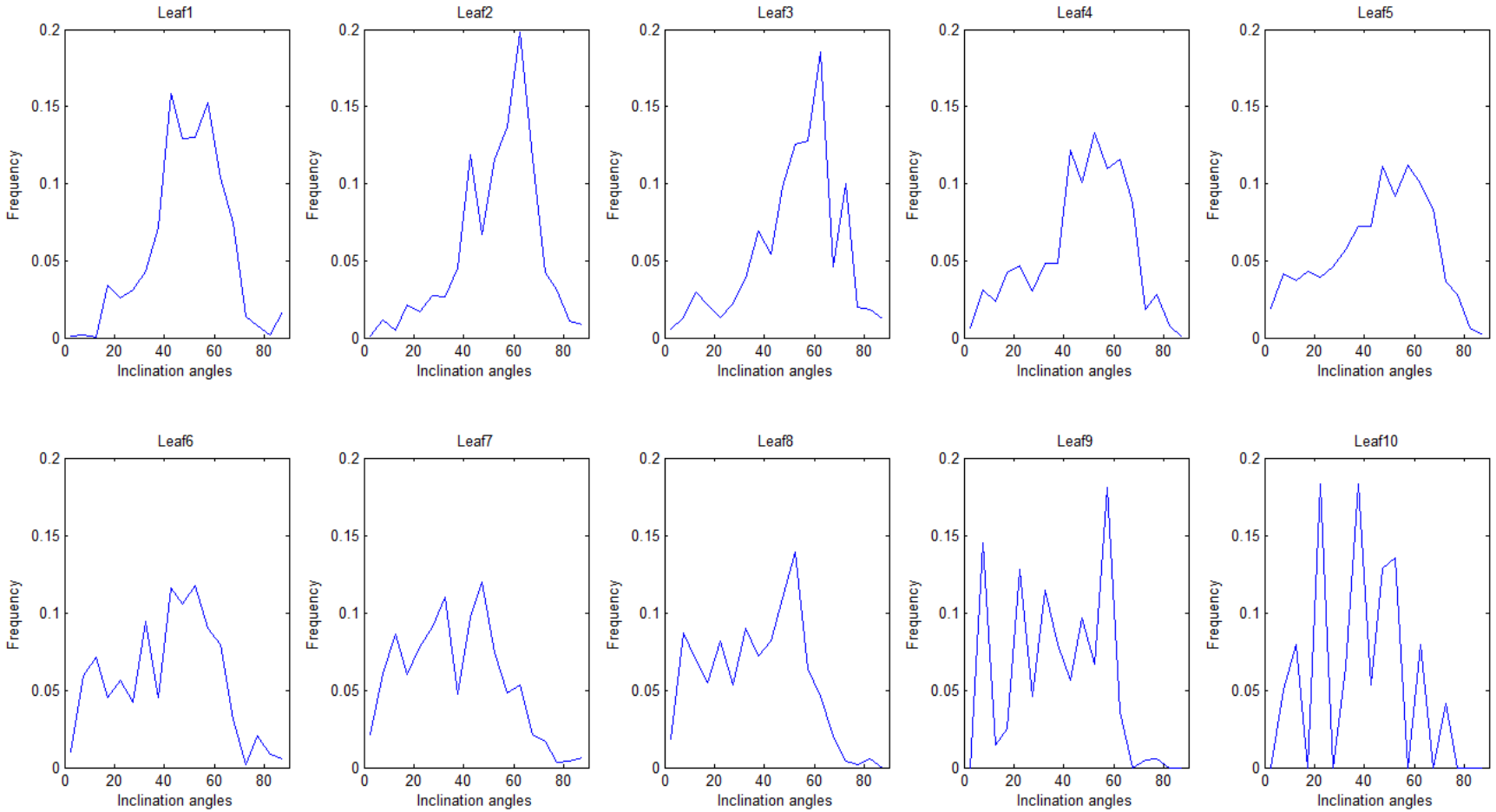

Figure 9 LAD of vertical profile for all sample plants

3.3 Reflectance of SLC model

No matter how sun zenith angle and viewing zenith angle change, reflectance in green (G) and red (R) band is always higher at low LAI than at high LAI level, whereas the opposite is seen in near infrared (NIR) that higher LAI result in higher reflectance (Figure 10 and 11). Reflectance of category 6, which is planophile canopy type, is always biggest regardless of each sun zenith angle and viewing zenith angle. In addition, the variation of reflectance related to the changing angle in category 6 is the smallest among all categories. The response of reflectance to increasing sun angle is non-linear, as both R and G bands see increasing reflectance whereas small fluctuation is seen in NIR. Especially at high LAI level, fluctuation is obvious in both G and NIR (Figure 10). However, linear trends are observed in increasing viewing angle regardless of LAI level as reflectance rises in all three bands (Figure 11). Besides, we can see the reflectance obtained from the azimuth angle 45° is higher than that at 135°. Planophile type also result in higher NDVI values, especially at lower LAI level. When the LAI is big, NDVI is not so much affected by different canopy type anymore (Figure 12).

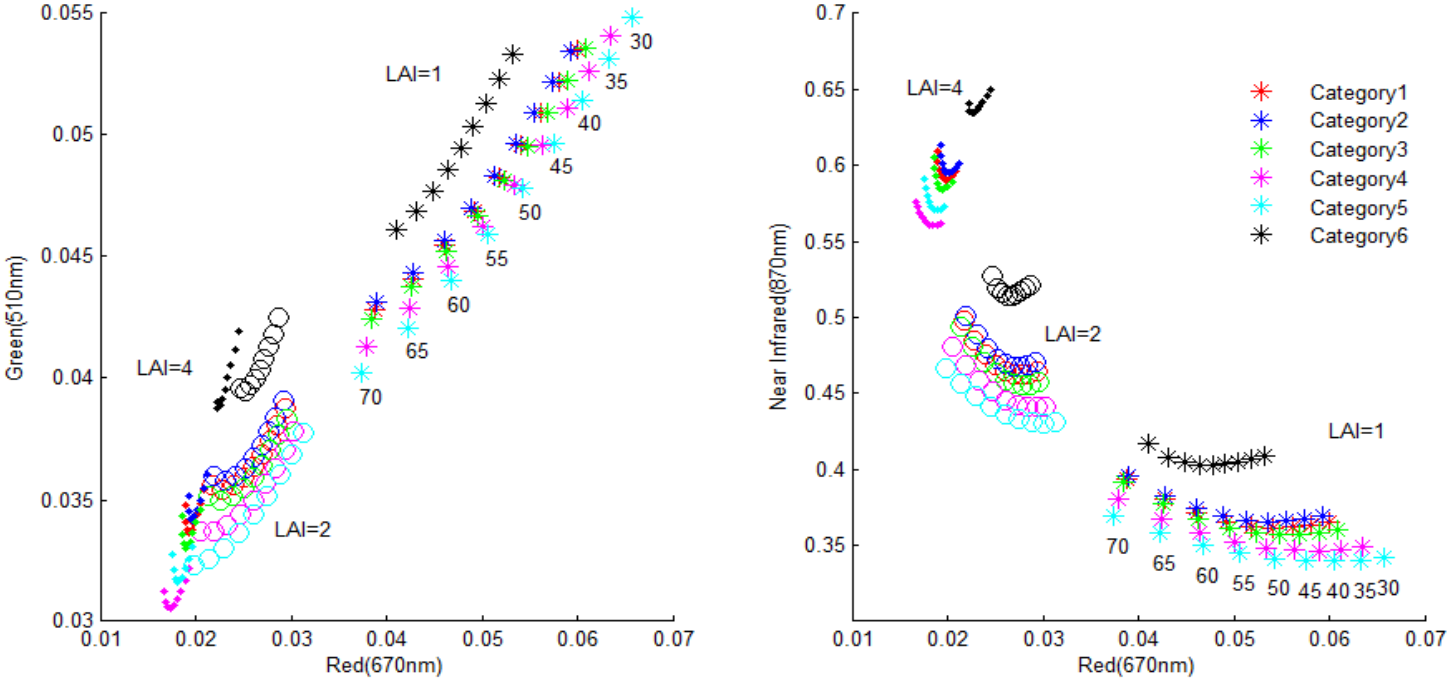

Figure 10 Influence of changing sun zenith angle on reflectance for 6 categories at different LAI level (viewing angle is nadir direction)

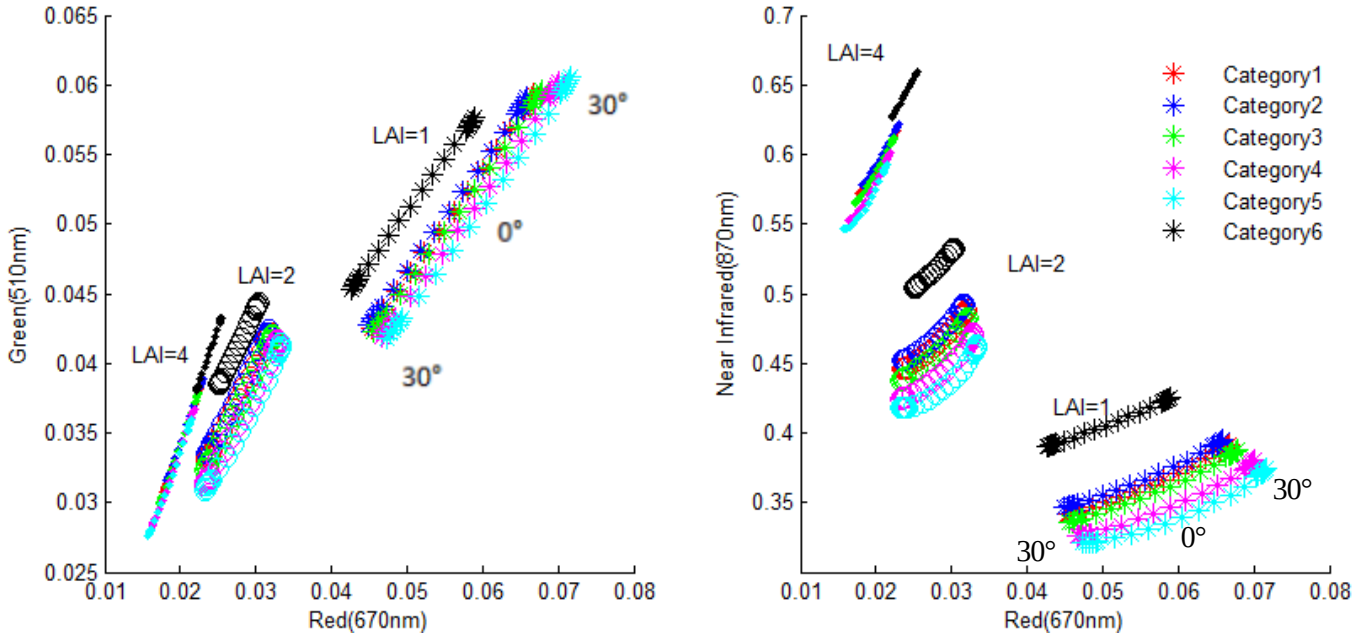

Figure 11 Influence of changing viewing angle (0°-30°) on reflectance of at different LAI level

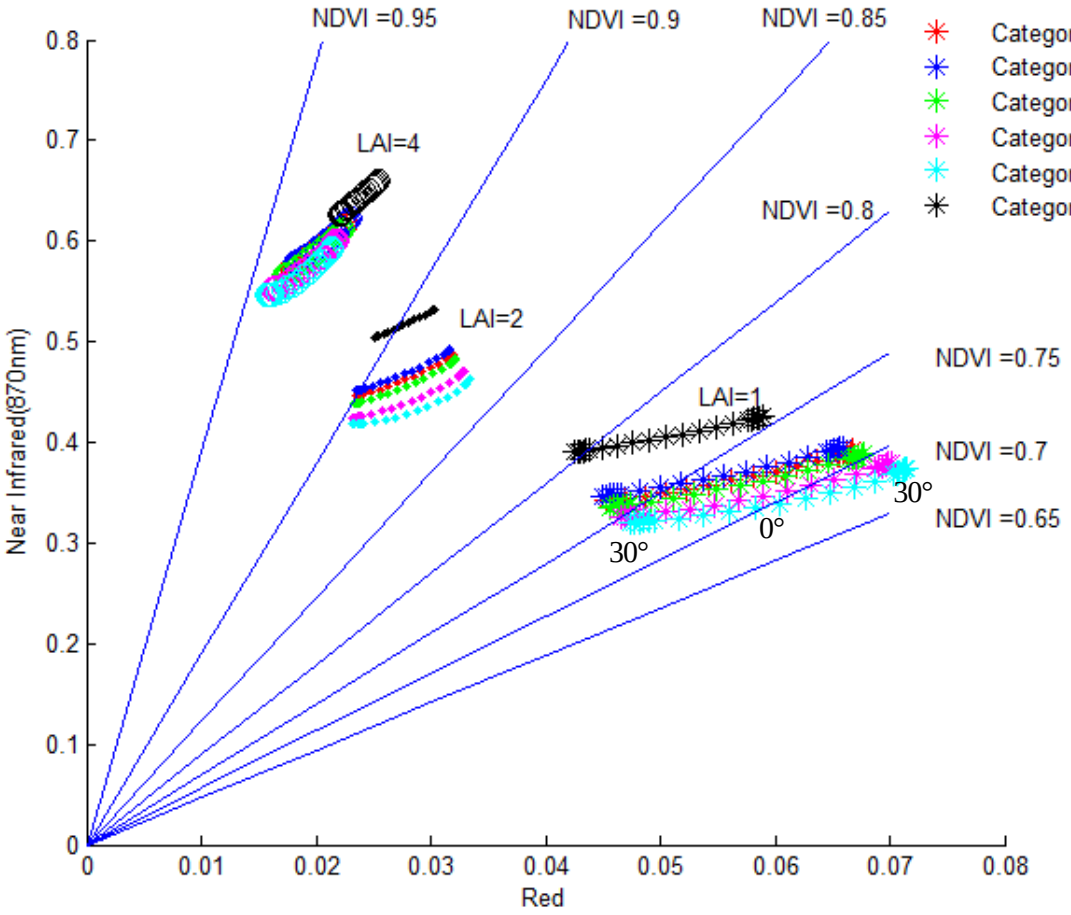

Figure 12 NDVI values of different categories at different LAI level

When LAI level is high, the ground is most covered by vegetation, and the sensor mostly observes vegetation that has reflectance property of strong absorption in G and R, and high reflection in NIR. However, when LAI is low, more soil surface is exposed and observed by the sensor. Soil has a higher reflectance in G and R than vegetation but much lower reflectance in NIR (Figure 25 in appendix). The Leaf angles then further affect how much soil is covered and shaded. The planophile canopy has most horizontal leaves, compared with plagiophile canopy, it covers more soil ground; therefore, the optical remote sensing observers see more vegetation instead of a mix of vegetation and soil in different viewing angles. This explains the small variation of reflectance in planophile canopy regardless of viewing angle or sun angle. As in the case of plagiophile, when the viewing angle changes, the proportion of vegetation and soil that is observed changes correspondingly which leading to a bigger variation in reflectance.

3.4 LIDF

3.4.1 Parameter retrieval of LIDF

The retrieved parameters using fitted distributions have good agreement with the parameters derived through fitting manual measurement (Table 10), which means the fitting is correct. For beta distribution, μ and ν have equal retrieval residues for all categories. The largest deviation is 1.07% (category 6) while the smallest is 0.07% (category 3). Regarding trigonometric function, retrieved parameter *b* produces small error than parameter *a* generally. The retrieved error in b is from 0.70% (category 2) to 1.90% (category 6), while it is from 0.25% (category 6) to 28% (category 4) in *a*. Ellipsoidal distribution and rotated-ellipsoidal distribution show quite similar behavior with biggest deviation seen in category 6 (2.95% and 9.28%) and smallest in category 4 (0.39% and 0.33%).

(1) Beta distribution

According to previous studies, μ has a strong negative correlation with mean leaf inclination angle while ν is not correlated (Zou et al., 2014). This relationship is also found in maize canopy (Figure 13), and the correlation coefficient R is up to -0.95. The parameter μ has bigger value in planophile type canopy. The correlation study on the μ and ν values (Table 9) reveals that correlation mechanism might behave quite similar for planophile and erectophile as the data trends are identical, and the systematic deviation is caused by mean leaf angle. In planophile the μ is bigger than ν and the opposite is seen in erectophile. The plagiophile group illustrates that the parameter μ and ν are about the same.

Table 9 Correlation between parameter μ and ν for different canopy type[2]

[2] The data is from the study on 58 broadleaf tree species (Pisek et al., 2013)

	Planophile	Plagiophile	Erectophile	uniform	spherical
R	0.88979	0.84414	0.99128	0.95884	-0.12125
Slope	0.36	**1.1**	0.56	2	0.043

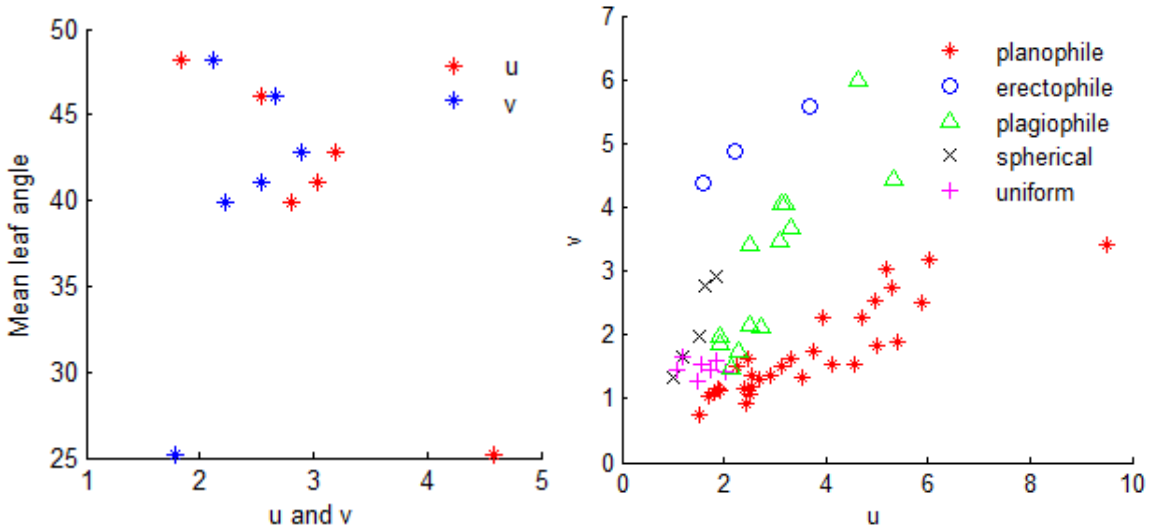

Figure 13 Correlation between parameter μ, ν and mean leaf angle of beta distribution

(2) Trigonometric function

In trigonometric function, the parameter *a* indicates the mean leaf angle while the parameter *b* indicates the bimodality of the leaf angle density (Verhoef, 1997). The *a* from the first 5 categories are close to 0, which means the mean angle are around 45°. This shows agreement with the statistics derived from manual measurement in Table 7. Bigger *a* value indicates the leaf is more horizontal, which is the case of category 6. The *b* value does not differ so much across all categories as only one peak presented in the fitted distribution of each category (Figure 14).

(3) Ellipsoidal and rotated-ellipsoidal distribution

The fitted parameter confirmed with study done by Thomas & Winner (2000). According to their study, parameter χ for the planophile leaf is large than 1 in ellipsoidal distribution and smaller than 1 in rotated-ellipsoidal distribution. The category 6 are dominated by planophile type, thus the fitted parameter χ behaves as expected. In Campbell's work (1986), the parameter χ is 1.37 when fitting the ellipsoidal distribution to maize canopy, which are also found in case of category 5. Parameter χ for plagiophile type (categories 1 – 5) falls within 1 to 2 for both distributions.

3.4.2 Fitted distribution

According to the fitting statistics shown in Table 11 and 12, the two-parameter functions outperform one-parameter functions. This is in good agreement with the study on tree species done by Wang et al. (2007). Beta distribution yields mean leaf angle closest to measured results, and the standard deviation of all categories is the smallest among all LIDFs. Trigonometric function is the second best approximations according to mean and standard deviation. However, in terms of fitting RMSE, trigonometric function yields the smallest error and is better than beta distribution. Between the one parameter functions, despite that both distributions produce quite similar mean angle in all categories, rotated-ellipsoidal distribution performs slightly better than ellipsoidal distribution with lower standard deviation and RMSE, which confirms the study done by Thomas and Winner (2000). Since uniform distribution and spherical distribution do not have any parameter, the estimated mean and standard deviation remains the same for all categories, which results in large deviations when compared with the measurement. The mean inclination angles estimated from uniform distribution however is closer to the measured than those from spherical distribution and also has lower RMSE, which consist with inclination index in section 3.1 (Table 7).

The two parameter functions outperformed the others are again confirmed in Figure 14. Both functions capture the trend of each category closely. Trigonometric function successfully predicts all the peak values of each distribution whereas beta distribution largely underestimates the peaks. For categories 1-5, beta distribution constantly overestimates the frequencies of angles around 20°-40°. Overall, according to visual examination, trigonometric distribution gives better fits than beta distribution, which is consistent with the RMSE data in Table 12.

Between one-parameter distributions, regarding categories 1-5, though both function failed to capture the trend, rotate-ellipsoidal distribution still fits slightly better than ellipsoidal distribution in categories 3 – 6 (Figure 14). It predicts the frequency peaks at around 40° - 60° successfully in spite of underestimating the peak values. Ellipsoidal distribution fails to predict the peaks by presenting a false peak value around 20°- 30°. The behavior of failing to predict peak values is also seen in Campbell (1986)'s work on maize. Besides, ellipsoidal distribution largely overestimates the frequency of leaf angles near 20° and 70°, which was also found in the study done by Thomas and Winner (2000). Both distributions tend to overestimate the frequencies at around 65° - 85°. In the case of category 6 (planophile type), the performance of both functions is much better than in the first 5 categories (plagiophile canopy type). Figure 10 shows that in category 6 they predict the peak correctly and capture the overall trend of the measured data despite that underestimation is observed at angle 30° - 40°. Rotated-ellipsoid failed to estimate the frequency at 0° - 5° bin due to its inherit property. Originally it is adjusted to improve the fitting by avoiding zero frequency at 0° (the case of

horizontal foliage), which might work for some tree species (Thomas & Winner, 2000). However, in case of maize, very small density is seen for angle between 0°-5°.

Table 10 Retrieved parameters of LIDFs

	Beta distribution				Trigonometric function				Ellipsoidal		Rotated Ellipsoidal	
	u	v	u'	v'	a	b	a'	b'	Chi	Chi'	Chi	Chi'
category 1	3.0310	2.5474	3.0272	2.5442	0.1036	-0.4744	0.0975	-0.4662	1.8326	1.8546	1.3493	1.3293
category 2	2.8021	2.2297	2.7931	2.2225	0.1428	-0.4582	0.1377	-0.4546	1.9215	1.9509	1.2850	1.2595
category 3	3.1898	2.8881	3.1890	2.8874	0.0588	-0.5054	0.0469	-0.4887	1.7175	1.7297	1.4418	1.4298
category 4	2.5506	2.6723	2.5466	2.6681	-0.0371	-0.4401	-0.0476	-0.4285	1.5107	1.5048	1.6400	1.6454
category 5	1.8424	2.1273	1.8275	2.1101	-0.1019	-0.3071	-0.1063	-0.3077	1.3860	1.3691	1.7853	1.8034
category 6	4.5925	1.7847	4.5433	1.7656	0.5447	-0.4031	0.5433	-0.3955	3.5023	3.6056	0.6667	0.6048

Table 11 Statistics of measured LAD and fitted LAD

	Measured		Uniform		Spherical		Ellipsoidal		Rotated-Ellipsoidal		Beta		Trigonometric	
	Mean	SD	Mean	SD	Mean	SD	Mean	SD	Mean	SD	Mean	SD	Mean	SD
Category 1	41.10	17.48	45.00	25.94	57.26	21.55	40.79	23.26	40.73	23.00	**41.09**	17.49	41.44	18.06
Category 2	39.88	18.20	45.00	25.94	57.26	21.55	39.49	23.19	39.39	22.84	**39.86**	18.23	40.03	18.30
Category 3	42.77	16.89	45.00	25.94	57.26	21.55	42.58	23.31	42.56	23.17	**42.76**	16.90	43.32	17.71
Category 4	46.05	18.03	45.00	25.94	57.26	21.55	46.15	23.25	46.13	23.32	**46.05**	18.05	46.67	18.70
Category 5	48.23	20.13	45.00	25.94	57.26	21.55	48.54	23.07	48.49	23.29	**48.27**	20.20	48.68	20.59
Category 6	25.19	14.88	45.00	25.94	57.26	21.55	24.54	20.02	23.34	18.24	**25.05**	14.94	25.23	15.15

Table 12 RMSE of LAD using fitted LIDFs

	Uniform	Spherical	Ellipsoidal	Rotated-Ellipsoidal	Beta	Trigonometric
Category 1	0.0409	0.0498	0.0368	0.0322	0.0217	**0.0103**
Category 2	0.0410	0.0517	0.0369	0.0335	0.0245	**0.0070**
Category 3	0.0451	0.0511	0.0414	0.0358	0.0265	**0.0154**
Category 4	0.0454	0.0479	0.0422	0.0357	0.0304	**0.0163**
Category 5	0.0345	0.0355	0.0311	0.0224	0.0220	**0.0117**
Category 6	0.0528	0.0756	0.0323	0.0342	0.0186	**0.0104**

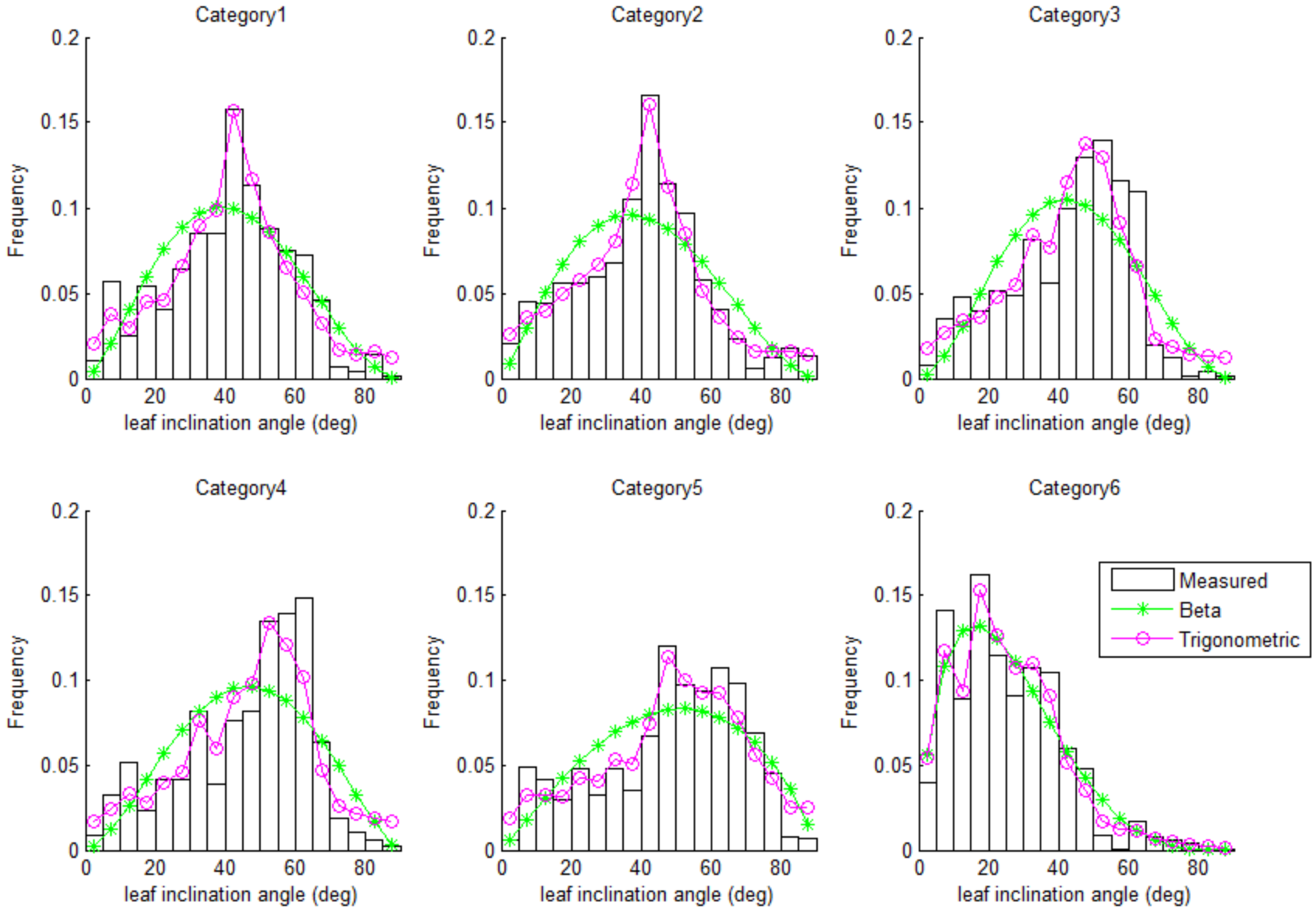
Category1
Category2
Category3
Category4
Category5
Category6
Frequency
leaf inclination angle (deg)
0
0.05
0.1
0.15
0.2
0
20
40
60
80
Measured
Beta
Trigonometric

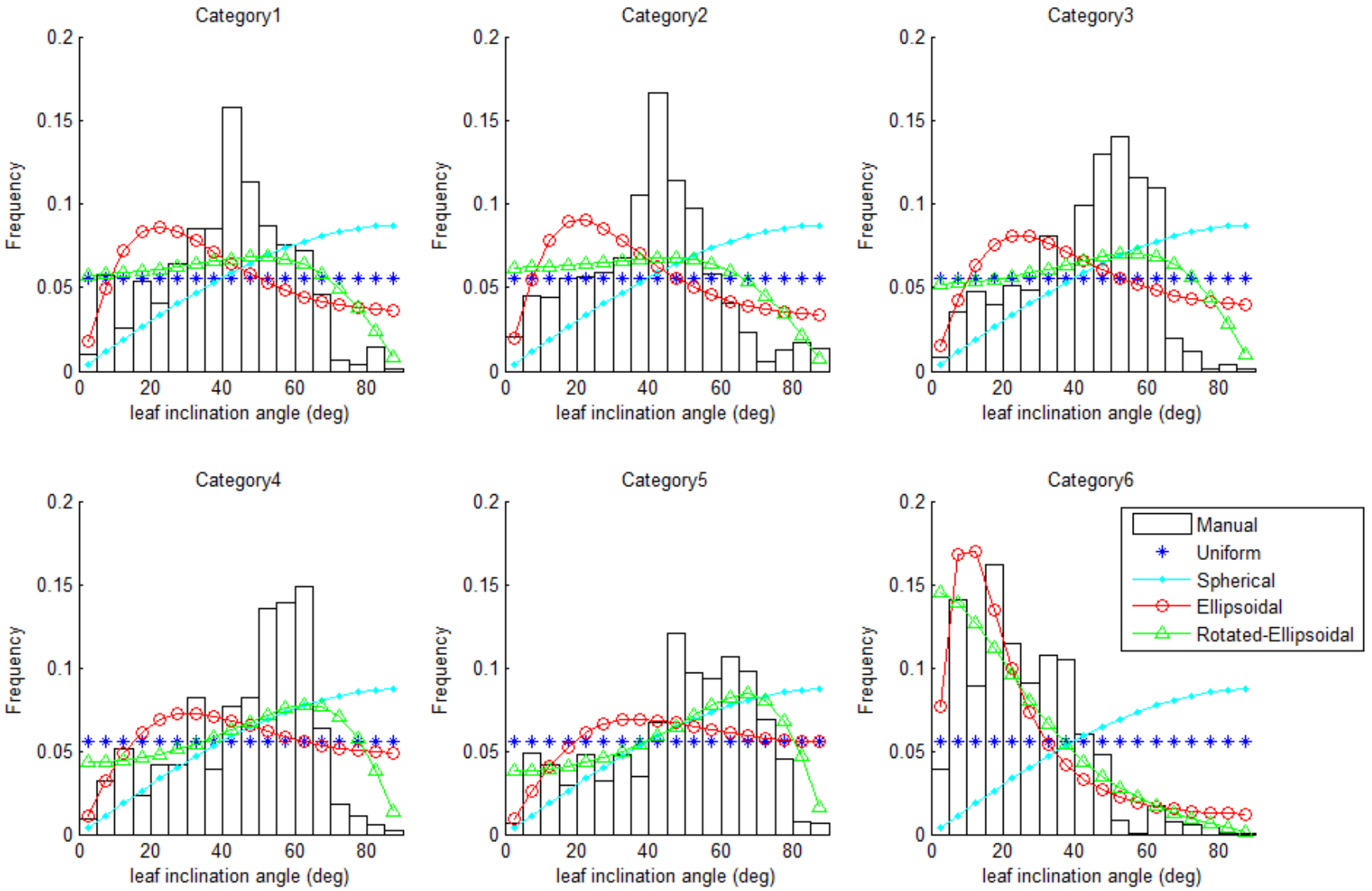

Figure 14 LAD of fitted LIDFs

3.5 G, K and LAI

The G function plot (Figure 15) shows that both one-parameter and two-parameter LIDFs generate quite similar results despite the large difference in LAD. Thus some compensate effect presents during calculating G using LIDF. For category 2 and 6, plagiophile and planophile behavior are as expected. Especially for later, the measured and fitted have good agreement. Among all LIDFs, Beta distribution and trigonometric function produce G values that highly consistent with manual measured results.

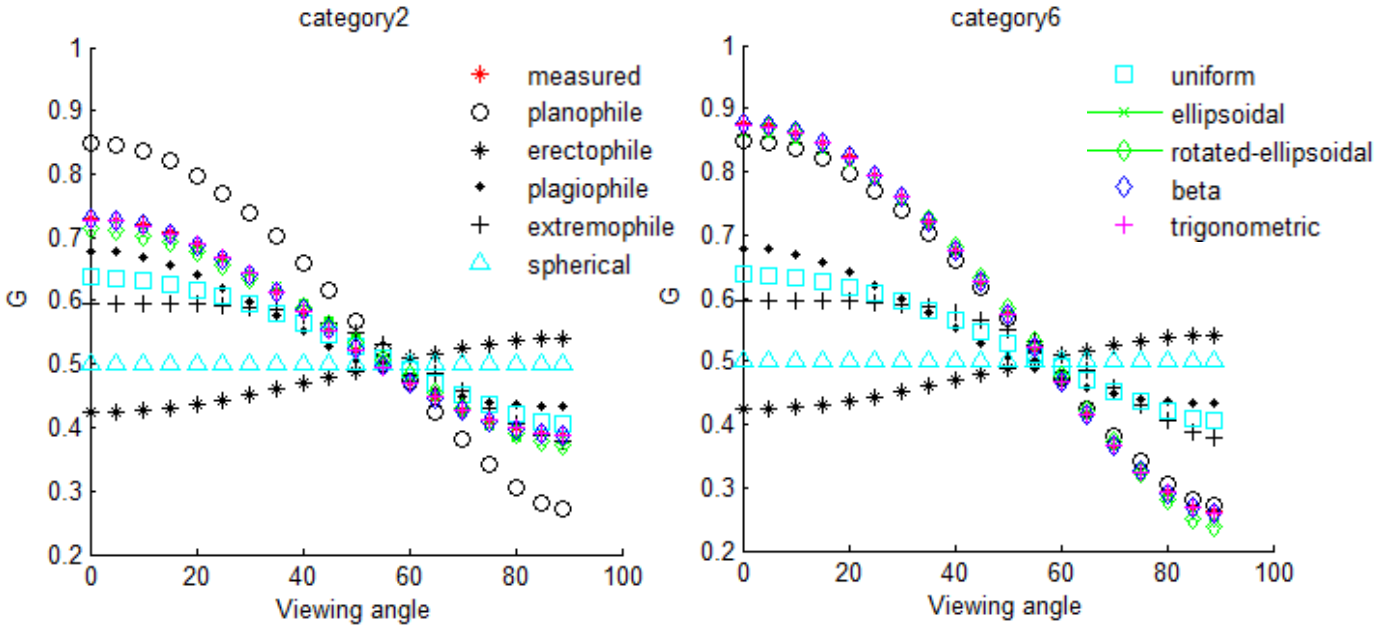

Figure 15 G function calculated using different LIDF for category 2 and category 6

All G values come across at a viewing angle of around 57°. However, they do not necessarily intersect at the same viewing angle 57.5° and variations are seen (Figure 16). The G value residue (viewing angle from 50° to 65°) implies that the parametric LIDFs have much smaller residues than the non-parametric LIDFs. The biggest deviation from measured result is 3.92% (erectophile) from category 1 while the smallest is 0.05% (trigonometric function) from category 6. Overall, the G value residue around this angle is small despite of assuming different LIDFs.

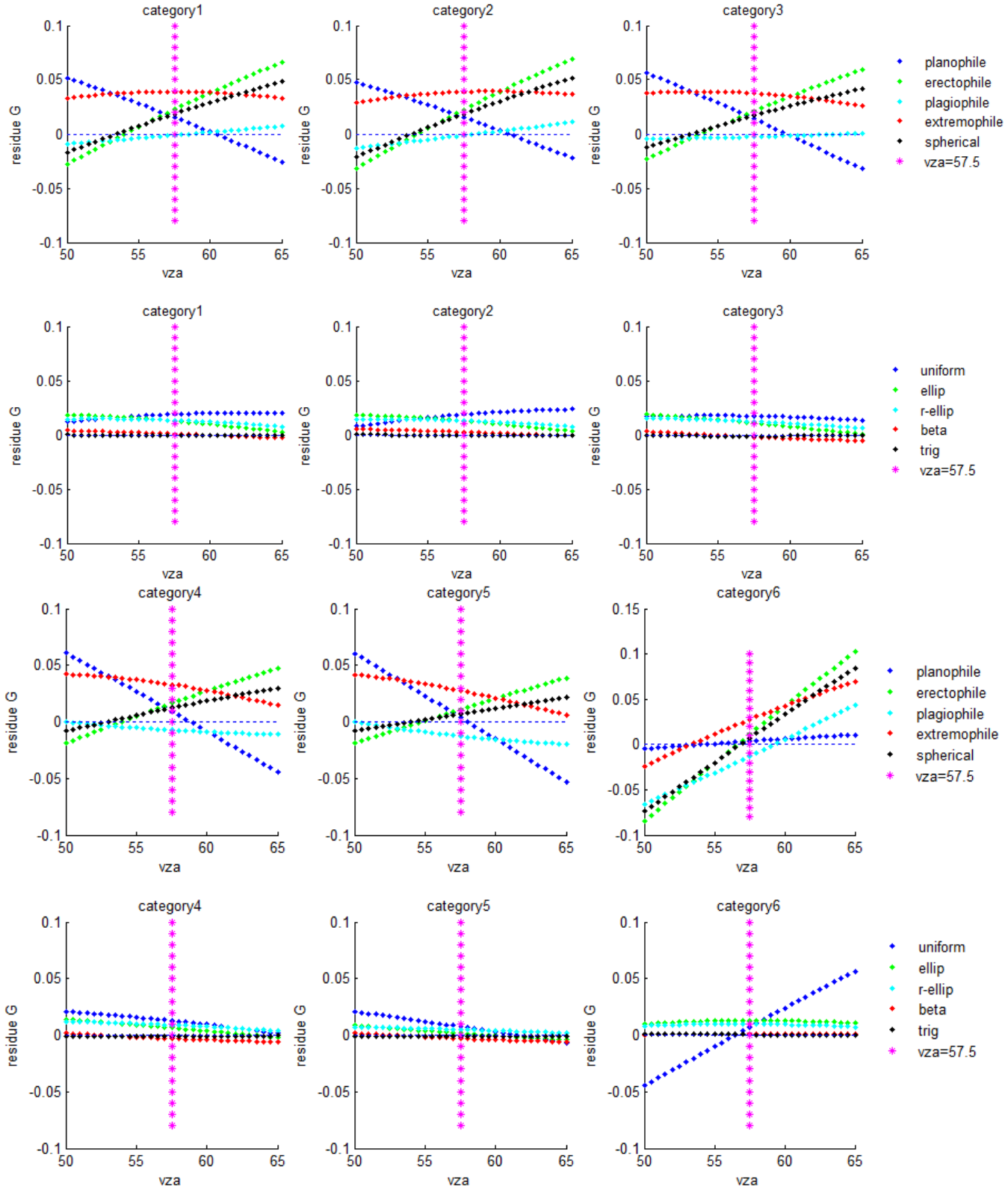

Figure 16 G residues using different LIDFs

When viewing zenith angle is between 0° to 70°, the effect of LAD/LIDF on extinction coefficient K estimate is small, which is also found in W.-M. Wang et al (2007)'s work. However, when viewing angle exceeds the range, K value increases dramatically (Figure 17). The same as G value residue, when viewing angle approaching 57.5°, K shows small variation among LIDFs (Table 13). When assuming a spherical distribution, K is 0.9306, which has been utilized widely in calculating LAI (Demarez et al., 2008; Liu et al., 2013; M. Weiss & Baret, 2014). It deviates from K value calculated using measured LAD from 1.1% to 4.4%. The planophile type has deviation from 0.88% up to 3.65% while plagiophile assumption keeps deviation under 0.30%. Ellipsoidal distribution has deviation from 0.31% to 0.39% while rotated ellipsoidal distribution is from 0.32% to 1.16%. Beta distribution controls the deviation under 0.73%. The best performance is seen in trigonometric function with biggest residue being 0.27%.

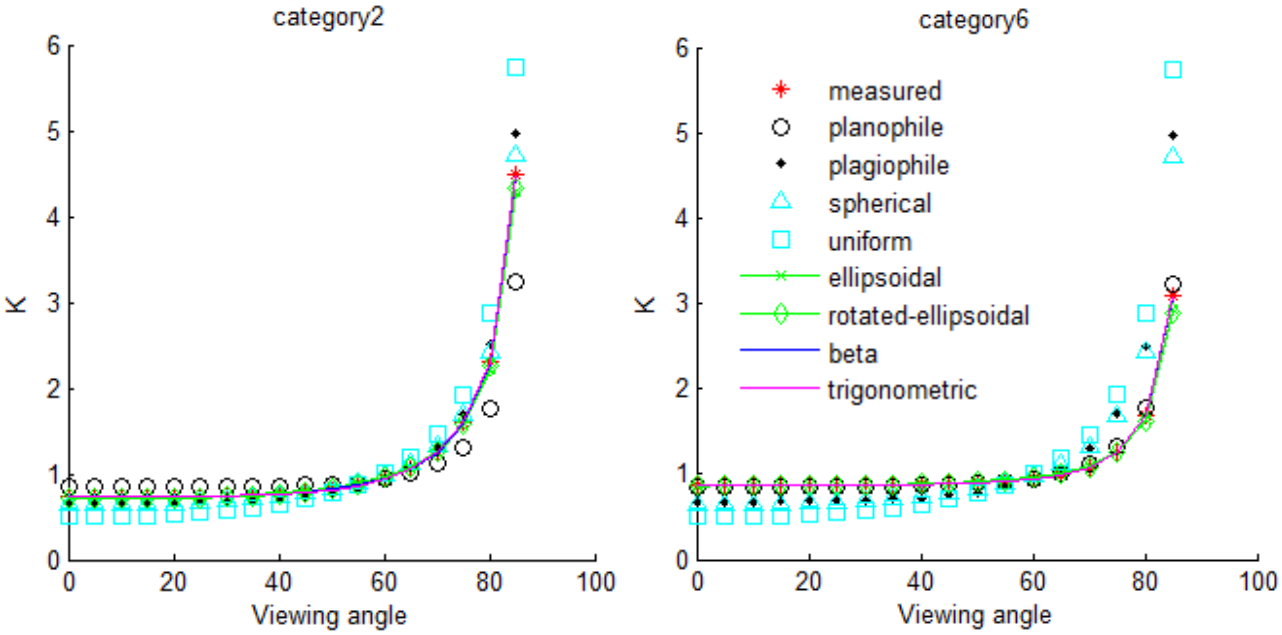

Figure 17 Extinction coefficient K derived using different LIDFs for category 2 and 6

Table 13 Extinction coefficient K derived using manual measurement and LIDFs at viewing angle 57.5°

	Manual	Plano-phile	Plagio-phile	Spherical	Uniform	Ellip-soidal	Rotated Ellipsoidal	Beta	Trigo-nometric
Category 1	**0.8960**	0.9247	0.8939	**0.9306**	0.9314	0.9198	0.9210	0.8976	0.8951
Category 2	**0.8964**	0.9247	0.8939	**0.9306**	0.9314	0.9204	0.9207	0.9010	0.8953
Category 3	**0.8989**	0.9247	0.8939	**0.9306**	0.9314	0.9193	0.9218	0.8952	0.8970
Category 4	**0.9075**	0.9247	0.8939	**0.9306**	0.9314	0.9196	0.9244	0.9018	0.9054
Category 5	**0.9176**	0.9247	0.8939	**0.9306**	0.9314	0.9207	0.9267	0.9120	0.9155
Category 6	**0.9178**	0.9247	0.8939	**0.9306**	0.9314	0.9419	0.9362	0.9201	0.9186

As the viewing angle of gap fraction changes from 50° to 59°, the RMSE of LAI (category 2) retrieved using non-parametric LIDFs varies more than using parametric LIDFs (Figure 18). Regarding parametric distribtuion derived LAI, trignometric distribution has negligible errors (0.00%-0.14%) at

all viewing angles, and beta distribution sees the biggest error 1.02%. Both rotated-ellipsoidal distribution and ellipsoidal distribution controls error under 3.56%. Regarding non-parametric LIDF derived LAI, as category 2 is subject to plagiophile canopy type, LAI calculated using plagiophile LIDF yields consistantly small errors (0.12% - 2.73%) across the viewing angles. The planophile, erectophile, and extremophile type, however, introduce much larger errors that can be up to 9.00%. The unfiorm distribution brings in error from 1.57% to 4.15%. Spherical distribution, the most used assumption, results in estimation error from 0.16% (at 54° viewing angle) and 4.49% (when viewing angle is away from 54°).

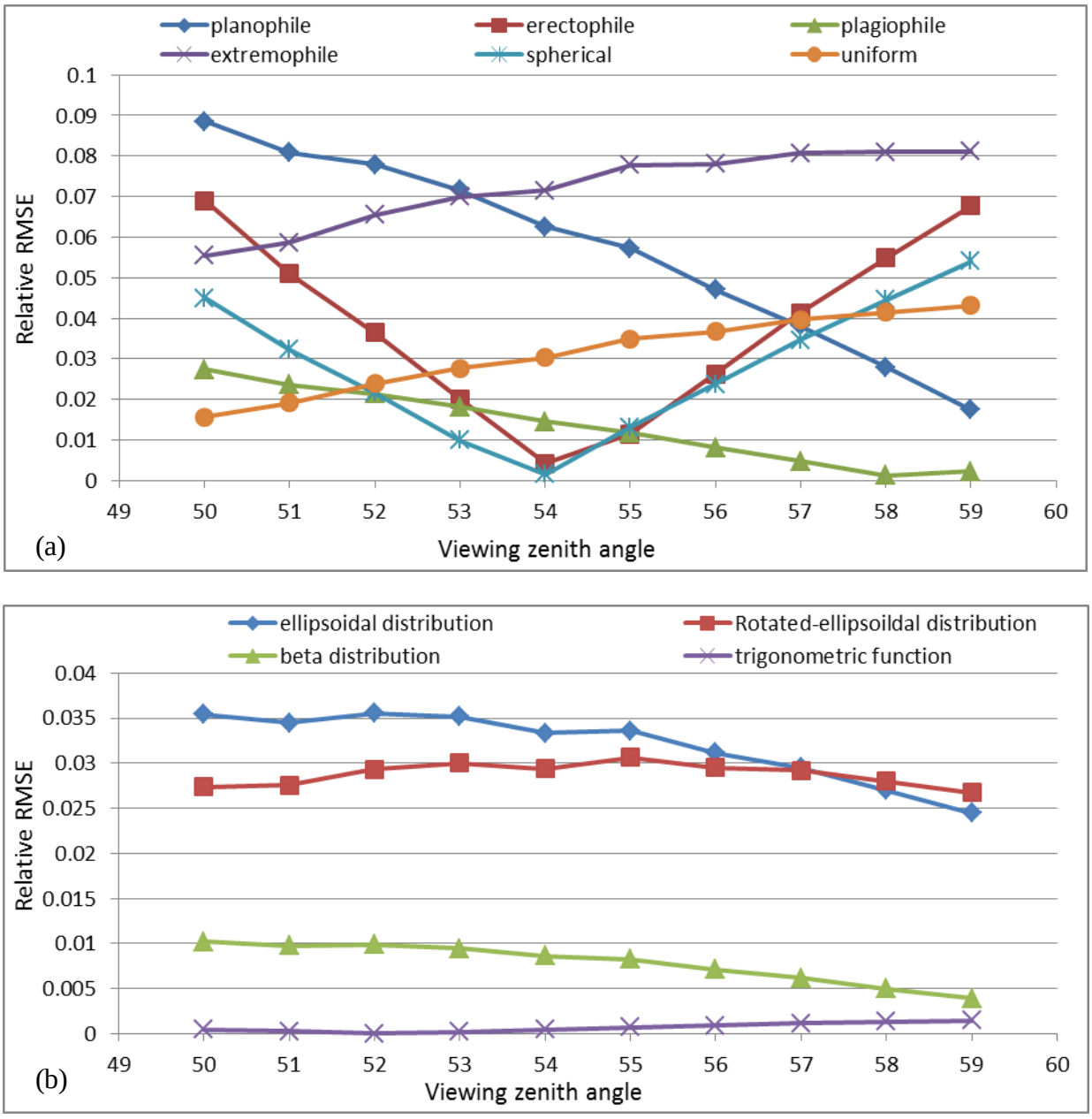

Figure 18 Relative RMSE of LAI in category 2 at viewing angles from 50° to 59°:
(a) LAI retrieved using Non-parametric LIDFs; (b) LAI retrieved using parametric LIDFs

3.6 DP measurement

3.6.1 Width function

The width is always largest at 1/3 or 1/4 relative length of a leaf (Figure 19(a)). The different categories have different leaf shape according to the width base function (Table 14), and the shape variation is bigger between category 1, 6 and the other three. The change of width along the leaf tip direction is smallest in category 1 as generally it has much smaller leaf size and length. Categories 2, 3 and 4 which are not significantly different in LAD according to test result (section 3.2) have quite similar leaf shape, and leaf width in category 3 is about 0.5 cm smaller than the other two. Category 1 and 6 shares similar shape parameter $c_{category}$, so are category 3 and 4. Category 2 has the biggest $c_{category}$ value (Table 14).

Validation of width function (Figure 19(b)) finds the biggest RMSE in category 2 (6.05cm) and the smallest in category 6 (2.11 cm). The errors are mainly produced around two ends of a leaf blade, near the stem and near the leaf tip. Despite big RMSE are seen, the modeled width are highly correlated with the measured leaf width in all categories, with correlation coefficient R larger than 0.91 in the first four categories and as high as 0.9854 in planophile canopy category 6 (Figure 19(b)).

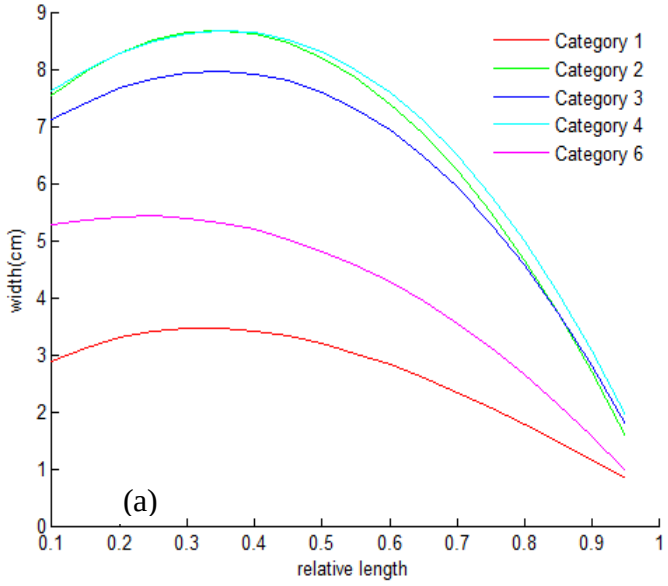

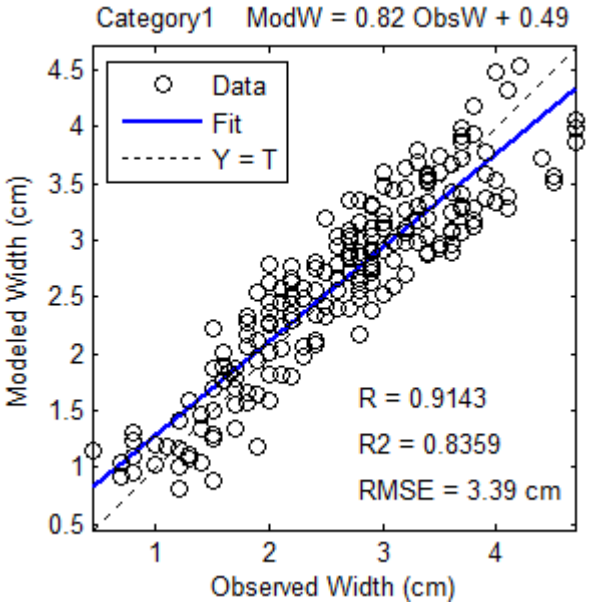

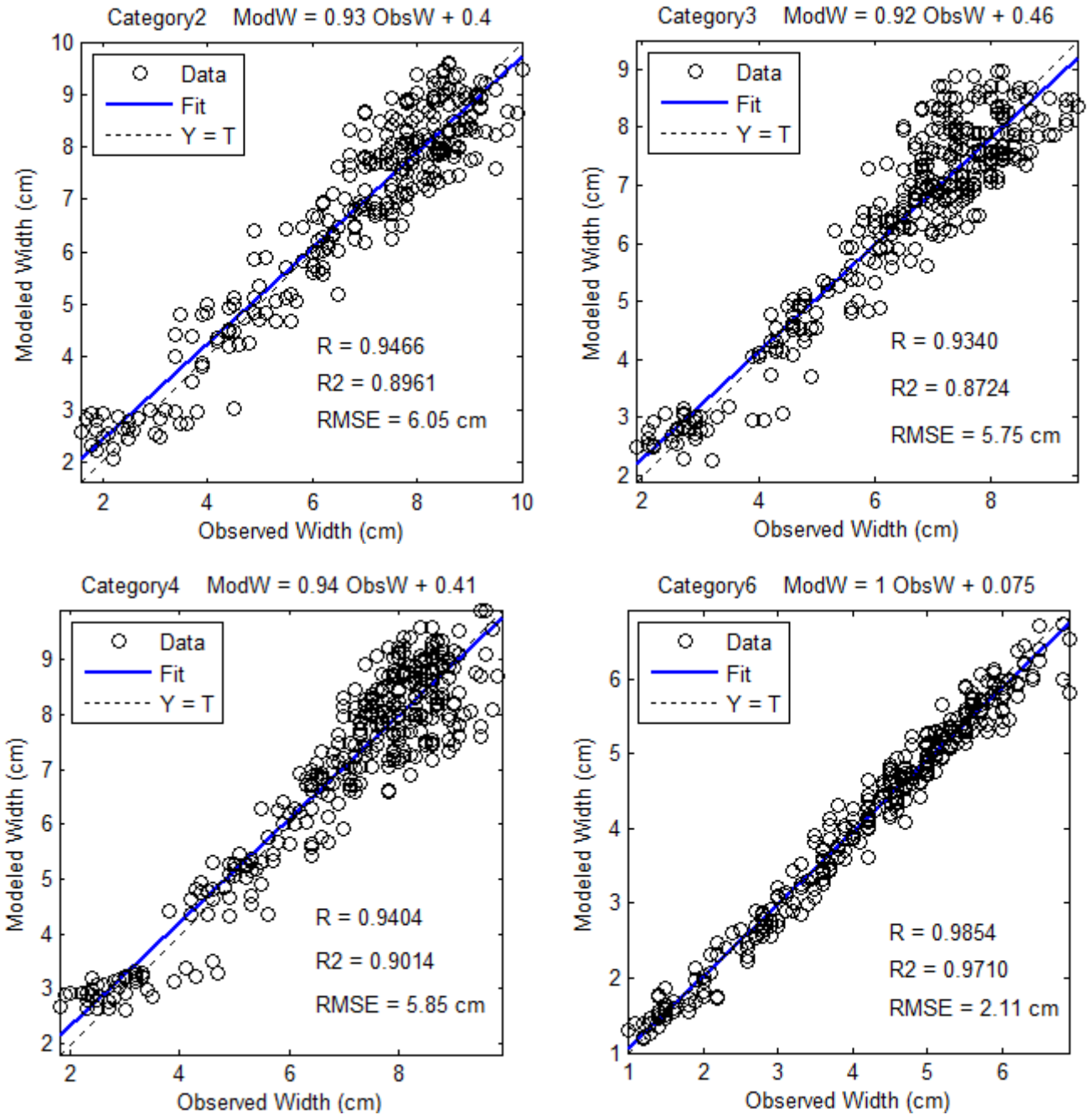

(b)

Figure 19 (a) width base function of 6 categories (b) regression plot of modeled and measured width for 5 categories (R2 stands for the coefficient of determination R^2).

Table 14 The polynomial function coefficients and shape adjust parameter $c_{category}$ of 6 categories using boot strap technique

	Category1	Category2	Category3	Category4	Category6
p_0	2.1409	6.2513	6.3394	6.5847	4.8787
p_1	7.8747	14.0111	9.2659	11.2968	4.4931
p_2	-14.3566	-21.3505	-12.0194	-14.4203	-9.5066
p_3	4.8275	1.3588	-2.8961	-2.824	0.4865
$c_{category}$	0.66	0.79	0.71	0.7	0.64

3.6.2 Area modeling

The modelled leaf area shows good agreement with observed ones as all R are above 0.9 (Figure 20). Especially in category 6, the modelled area is highly correlated with observation (R=0.99), which can be explained by the well modeled leaf width (Figure 19(b)). In spite of that, a slight overestimation in a systematic manner is seen in category 1 (4.4 cm^2) and 2 (10 cm^2), which is not shown in width modelling results. However, similar to the results obtained in width modeling, the biggest RMSE is found in category 2 (68.18 cm^2), and ranges from 4.11 cm^2 to 30.02 cm^2 for the rest categories.

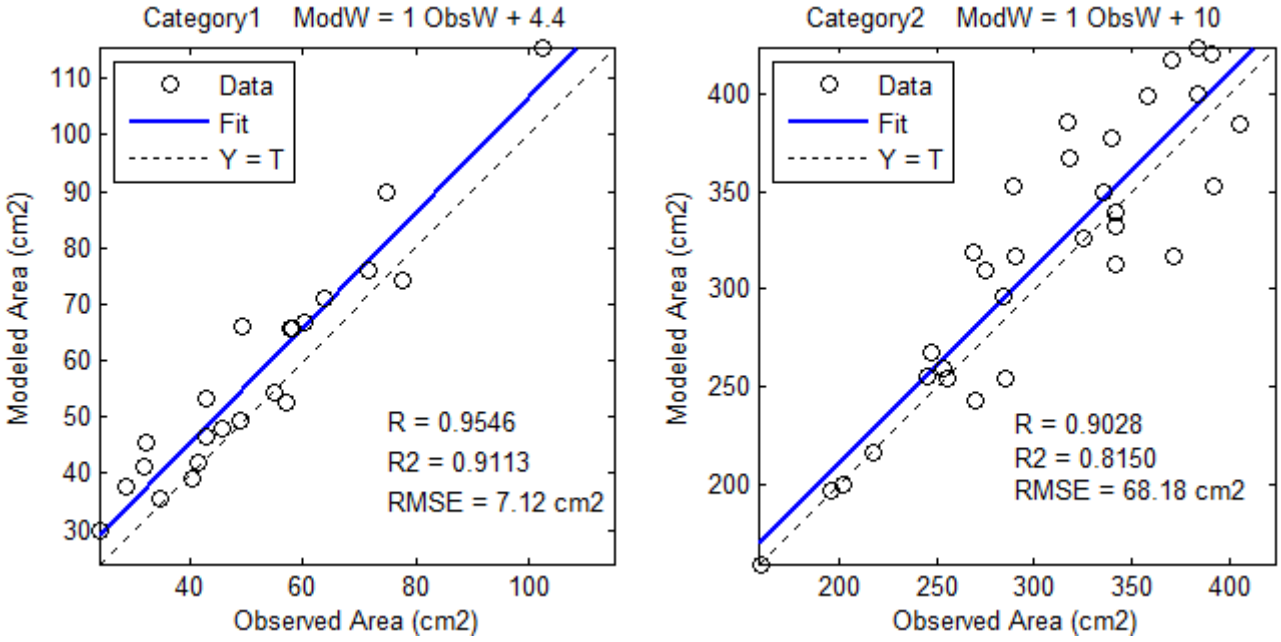

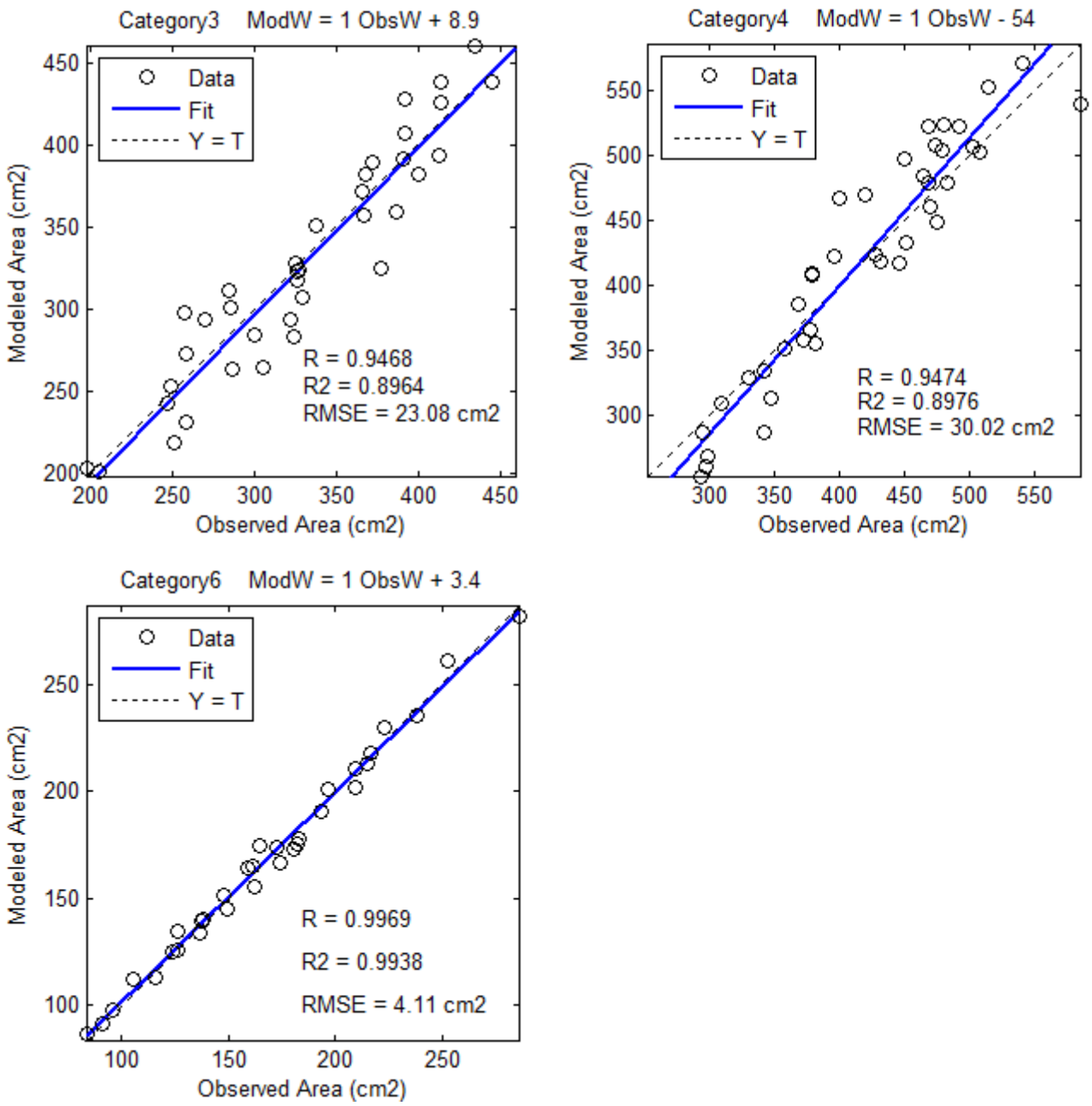

Figure 20 Validation of leaf area model for 5 categories.

3.6.3 LAD

The LAD derived from DP method captures the overall trend and successfully predicts the most frequent inclination angles in each category (Figure 21). In categories 1 and 2, DP measurement underestimates the peak values around 45°. In categories 1, 2 and 3, overestimation is seen between 7.5° -25°. Especially in category 2, an unusual peak value occurs around 7.5° from DP method, causing large deviation. Despite that, the visual examination demonstrates good fitness between the two methods.

The sampled angle number from DP method is slightly bigger than manual measurement (Table 15). The RMSE indicates good agreement for all categories, especially in case of category 6 (RMSE=2.37%). DP method underestimates mean leaf angles in all categories by 2°-4°. The variation of standard deviation, compared with manual measurement, is small (0.12°-2.68°). The A-D test results also point to the same direction, as the LAD identity of the two methods is accepted for all categories (P>0.60). It means the null hypothesis is accepted, and thus LAD retrieved using these two methods have no significant difference. Highest agreement is found in category 1 while lowest in category 3.

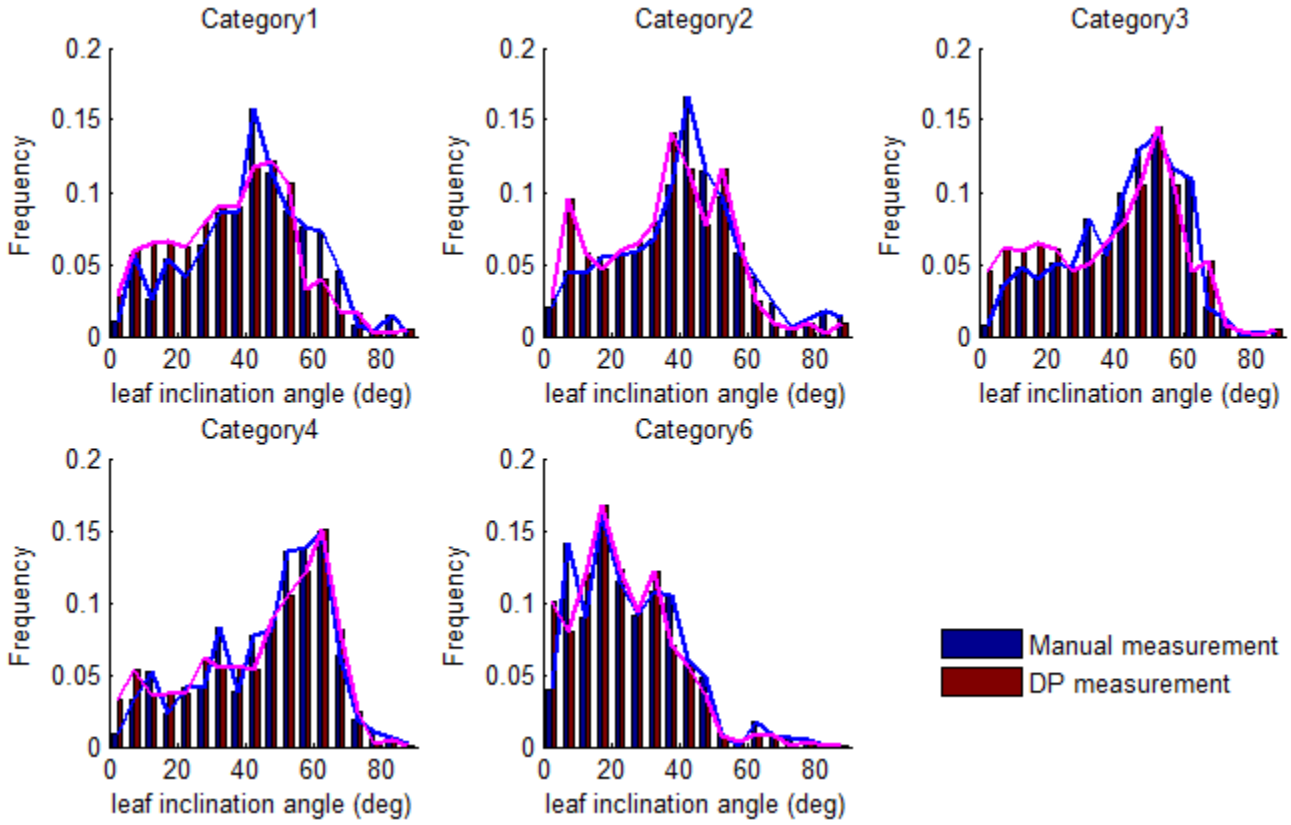

Figure 21 LAD from DP measurement

Table 15 DP measurement statistics

	Digital Photograph			Manual			RMSE	A-D test	
	count	Mean	SD	count	Mean	SD		D	P
Category1	322	36.23	17.60	269	41.1	17.48	0.0473	0.1786	**0.8118**
Category2	495	35.79	17.98	487	39.88	18.2	0.0485	0.4832	**0.6449**
Category3	512	38.76	19.57	446	42.77	16.89	0.0589	0.5464	**0.6062**
Category4	577	44.23	19.78	518	46.05	18.03	0.0697	0.5253	**0.6191**
Category6	207	23.22	14.07	201	25.19	14.88	0.0237	0.4886	**0.6416**

(Note: the confidence level is set to be 95%. When calculated p value is larger than 0.05, the null hypothesis is accepted.)

3.6.4 Influence on G, K and LAI

The calculated G function and extinction coefficient K based on the two LAD shows good agreement, especially for category 4 and category 6 (Figure 22). DP method overestimates G and K value when viewing angle is smaller than 60°, and underestimates when viewing angle is larer than that. The G residues of DP method for 5 categories are from 0 to 9.71%. Deviation is largest in category 1 , while for category 4 and 6, the deviation is under relative error 3.59% and 5.67% respectively (Figure 23). K value stays stable at viewing angle 0°- 40°, and changes rapidly as viewing angle increase from 40° onwards. Its residue decreases to 0 at viewing angle around 60° for all 5 categories. The farther away from this angle, the bigger the residue is, but they are all under 9.71% relative error. LAI calculated for category 2 using gap fraction at 57° viewing angle shows perfect agreement (Figure 24), and the RMSE of LAI derived using the rest viewing angles are from 0.20 % up to 3.00 %. At 57° viewing angle, the G residue is 0.56%, and K residue is 0.55%, and the retrieved LAI has a RMSE of 0.62%. The result suggest that LAI retrieved using LAD from DP method could achieve equivalent result as using manual measurement, especially when viewing angle is approaching 57°.

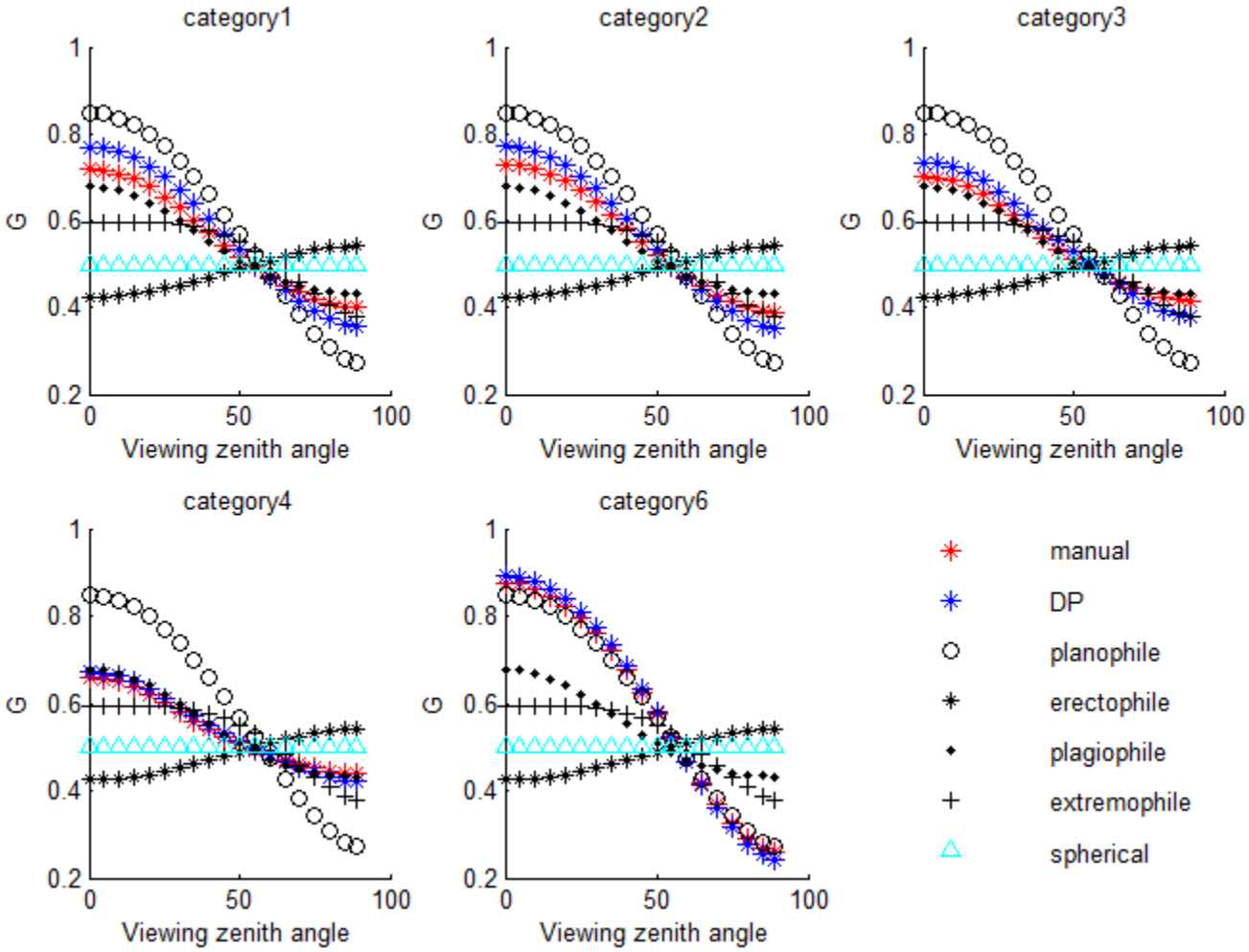

Figure 22 G function of 5 categories using LAD from manual measurement and DP method

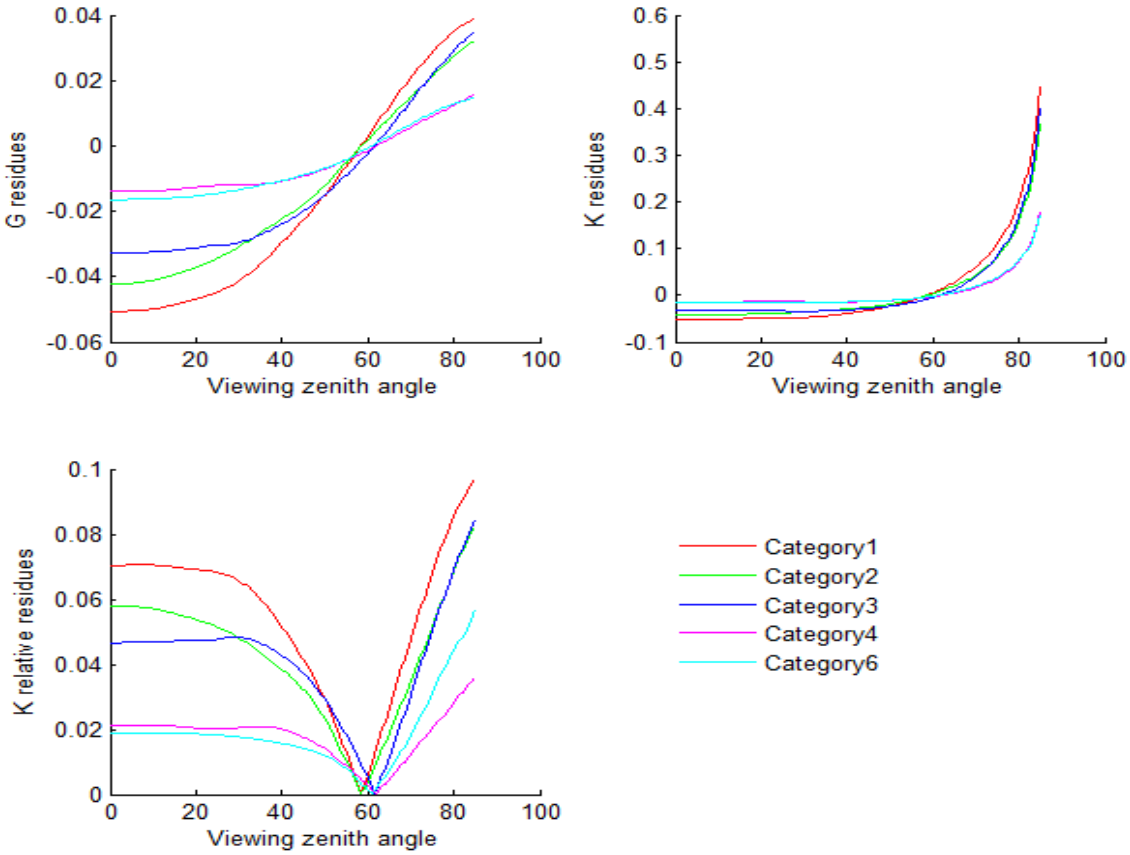

Figure 23 G residues and K residues between manual measurement and DP method for 5 categories

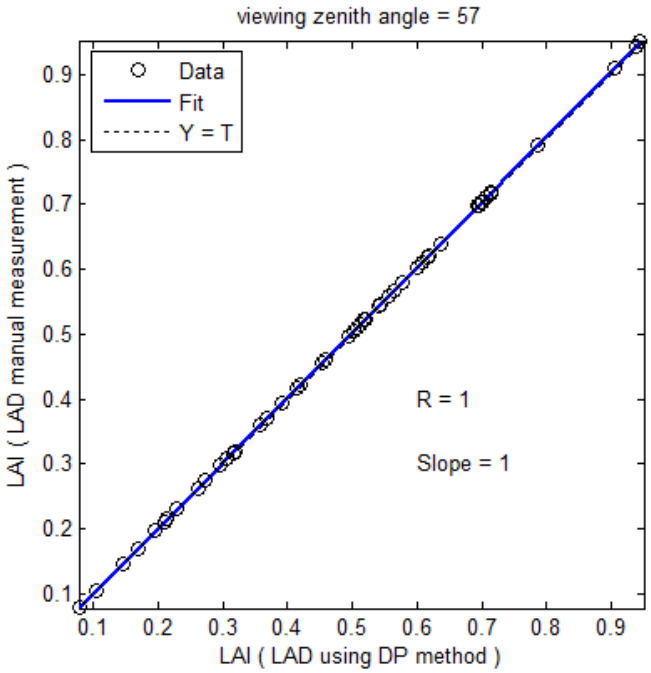

Figure 24 Regression plot of LAI derived at 57° viewing angle

3.6.5 Minimum sample size

Regarding manual measurement, different categories show different minimum sample size according to A-D test (Table 16). Planophile canopy (category 6) requires much smaller sample size than plagiophile canopy (categories 1-5). Reproductive maize canopy (categories 2-5) needs slightly more sample size than vegetative one (category 1). The A-D test results also indicate that DP method needs slightly larger sample size to generate LAD that would not significantly differ from manual measurement (Table 16). Overall, 1 or 2 more plants are needed for DP methods. DP method provides more sampled leaf angles than manual measurement since the leaf can be much more easily divided into as many segments as wanted on a photo than it is in the field.

Table 16 The minimum sample size of plant, leaf and inclination angles from manual measurement and DP method. The number is the minimum sample size that yields LAD not significantly differs from the manual measurement using original dataset at 95% confidence interval.

	Manual - Manual			Digital Photograph -Manual		
	Plants	Leaves	Angles	Plants	Leaves	Angles
Category1	10	72	176	11	75	248
Category2	14	111	294	15	113	338
Category3	11	77	246	13	93	329
Category4	11	83	270	13	96	374
Category5	11	92	310	-	-	-
Category6	7	36	82	8	42	104

4. Discussion

4.1 Different development stages and environmental conditions

The study finds that both vegetative stage maize plant (category 1) and reproductive maize plant (categories 2-5) have plagiophile canopy type, which means the majority of leaves are oblique. This confirms the study done by de Wit (1965) and Lemeur (1973). However, the A-D test result suggests that LAD of category 1 significantly differs from the remaining categories (p=0.00-0.03). This is caused by large sample size difference, which is illustrated in Table 17. As a result of suffering most from water logging, category 1 has an average height of around 0.45m, and average leaf area of 42.27 cm^2 (Figure 24 (a)) which is much smaller than the other categories. This results in the large difference in sample size compared with the other categories, because the leaf area was counted for the frequency of each leaf inclination angle (section 2.3). Though the A-D test does not require equal sample size, the huge variation (10 times variation in this study) of the tested dataset would always lead to a rejection of the null hypothesis. Despite the test result, the descriptive statistic and visual examination provide strong evidence that category 1 belongs to plagiophile canopy type and does not deviate from the categories 2 -5 much. Therefore, A-D test on canopy LAD has to be used with insights. In previous studies on tree species (Pisek et al., 2013), as a tree leaf only has one inclination angle, the angle number makes up the sample size. The A-D test in this case worked successfully. When it comes to a sample size composed of leaf area (such as most crop canopy), the A-D test may fail due to huge sample size variation. One way to address this problem is to transform the leaf area to be the same magnitude without changing the proportion in its angle bin. This adjustment was applied to category 1 by multiplying the leaf area of each angle bin with a constant to bring the sample size to the same magnitude as the other categories, and then the A-D test was performed again using the adjusted dataset. The test result shows no significant difference.

Regarding categories 2 to 5, the LAD difference is not significant (p=0.14-0.61), which means that they have similar LAD regardless of height. This may imply that the environmental conditions, soil nutrients and water logging, do not affect the LAD of maize plant. The previous study done by ZHANG et al. (2013) claims that nutrient and water supply conditions affect leaf inclination angles of rice crop. In this study, the mean leaf angles do increase as the plant height increases, but the LAD remains plagiophile type in all height groups.

Plagiophile type canopy has most occurrences in the field; however, it was unexpected that planophile type was also found in this study. Planophile canopy type has never been reported before for maize plants. All the plants were of the same hybrid and planted during the sample period. Planophile plants were in the late reproductive stages as categories 2-5 with an average height of 1.60m, but the leaf size was smaller (142.42 cm^2), and leaf area had small variation through vertical layers. Most plants have 5 -6 available leaves in this category. It is not clear what caused the large variation in maize canopy yet. But the planophile plants were mainly presented in the middle of the field where the overall canopy density was low.

As the field measurements were conducted in October when the weather condition was bad with lots of precipitation, most bottom leaves were dry and turned yellow or broken. Thus generally only 7 to 10 leaves were available for measurement. Therefore, the result might be biased due to the sample being in this condition, although the results are consistent with previous studies. The LAD result presented in this study cannot be generalized for maize plant. To better understand maize LAD variation across growing phase, it is recommended to mark the maize plants and measure the same plants during several key developing stages to investigate maize LAD. Since light interception varies during the growth cycle of maize (Lemeur, 1973; Loomis, Williams, Duncan, Dovrat, & Nunez A., 1968; G.A. Maddonni & Otegui, 1996), a detailed LAD information in each growing phase would help understand light interception in maize canopy better and in turn allow for better photosynthesis estimation. When using the A-D test to examine the significant difference, it is important to be aware of the sample size issue, and it is highly recommended to interpret the result with aid of visual examination of LAD or accumulative distribution plotting.

4.2 Vertical profile

Upper layers that present high density around 60° inclination angles are plagiophile type while the bottom layers are in between planophile and plagiophile type. However, this finding differs from Lemeur's work (1973) where bottom leaves are reported extremely plagiophile. The reason for this difference might be that the leaf layers are different. Since only 10 leaves are available in this study, the defined upper layer (leaf 1 -3), middle layer (leaf 4 -7) and bottom layer (leaf 8 – 10) might differ from Lemeur's (1973) definition if the studied maize from his work had more leaves. The LAD through the canopy layers can be explained by a plant growth strategy. The plagiophile type at the top allows more light to penetrate the canopy and reach the middle and bottom part, thus the use of radiation energy and in turn photosynthesis could be maximized. As the light penetration, interception and absorption through the canopy depend on the leaf angular distribution of leaf layers (Lemeur, 1973; de Wit, 1965), the vertical profile of LAD provides detailed information to simulate the processes.

4.3 Reflectance simulation using SLC

This study finds that planophile canopy type leads to higher reflectance in R, G and NIR than plagiophile canopy regardless of LAI value and higher NDVI values at lower LAI levels. Planophile canopy in which most leaves are horizontal; when compared with other canopy types, covers more soil area and intercepts more light regardless of sun angles. Furthermore, it also allows more of the leaf area to be observed by sensors no matter how the viewing zenith angle changes (except extreme cases such as 80°- 90°). This raises the awareness that, when using the optical remote sensing data to retrieve LAI, besides other biochemical content such as chlorophyll, canopy LAD also affects estimation results as demonstrated in the case of NDVI.

4.4 LIDF

The study confirms that two-parameter LIDFs, beta distribution and trigonometric function, appear to fit LAD much better in all cases. The previous studies demonstrate good performance of two-parameter LIDFs in simulating LAD of different tree species, but this study highlights their capability of characterizing a crop canopy that has completely different structure compared with trees. Wang et al. (2007) concluded that beta distribution is more appropriate than trigonometric distribution to simulate LAD. However, both visual examination and quantitative assessment in this study implies that improved trigonometric function yields the best performance among all LIDFs. The improved solution of the trigonometric function contributes to the low fitting RMSE. Trigonometric functions thus are highly recommended to be applied to simulate plant canopy. By varying parameter *a* and *b*, it has the capability of modelling all types of canopy LAD including the classical de Wit four types and spherical distribution.

The result indicates that ellipsoidal distribution and rotated-ellipsoidal distribution are more suitable for the planophile canopy type than the plagiophile type. In addition, together with the results from previous studies which apply these two distributions (Campbell, 1986; Thomas & Winner, 2000; W.-M. Wang et al., 2007), it is found that they give much better performance in estimating the planophile and erectophile canopy types. One parameter LIDFs, which use only mean leaf angle to derive parameter, is not enough to describe LAD that has bimodality or multiple high frequency angle clusters (W.-M. Wang et al., 2007).

4.5 LAI retrieval

The calculated G function and extinction coefficient K using different LIDFs show only small deviations despite that they produce different LAD. Therefore, some compensation effect exists in G and K calculation. When viewing angle approach 57°, all deviation decreases, and the estimated LAI shows good agreement for all LIDFs (relative RMSE is from 0.11% to 4.13%) except the extremophile type (relative RMSE is 8.07%). This result confirms previous studies that G function is independent of LIDF when having a viewing angle around 57.5°. Therefore, LAI can be retrieved accurately to some degree using parametric LIDFs or non-parametric LIDF that best approximates the plant canopy using gap fraction theory. However, further step of validating the result with destructive measurement of LAI has to be taken to make this determination.

4.6 DP methods

The 3rd order width function successfully predicts leaf width as a function of relative length. The results illustrate that vegetative stage maize plant (category 1) have different leaf shapes from the late reproductive stage plant (categories 2, 3 and 4), and the leaf shapes of plants from the same development stage are quite similar. The prediction error mainly occurs near the stem area and the tip area, as leaf width of these two areas have large variations while the width of the rest of the leaf changes more regularly and could be successfully modeled by using leaf shape parameter α. Compared

with a 4th polynomial used in the study done by Zou et al. (2014), a 3rd polynomial already has the power to produce satisfying results.

Modelled leaf area shows strong correlation with observation, especially in category 6 (planophile). The RMSE is much larger in categories 2, 3 and 4 than in the other two. This can be explained by the leaf blade character. The leaf size of those three categories is much larger and longer, and most middle and bottom layers are curved or even have waves. Besides, the mid rib causes the leaf on two sides form a small angle. This creates difficulties for leaf area measure operations as well as errors in using LAI3000. Leaves in category 1 and 6, however, are smaller and do not have this problem, which makes it much easier and more accurate to measure their leaf area.

The LAD derived from DP method does not significantly differ from manual measurements for all categories. The calculated G and K thus have very small deviation, which contributes to good LAI estimation (R is 1, and relative RMSE is 0.62%). The results indicate that the DP method can achieve equivalent and reliable LAD of maize canopy compared to manual measurements. This new approach provides some practical advantages over the other methods. Compared with an inclinometer or protractor, it is a non-contact method and is much more efficient to operate in the field. For example, during data collection, it generally took 20-30 minutes to measure all leaves of a plant manually, but only 3-5 minutes to take photos. Inclination angle measurement on the photos can also be done much faster than it is in the field. Compared with a laser scanner, it is much more affordable and flexible to use. Besides, it has been verified that the resolution of the camera does not affect the performance of the DP method (Pisek et al., 2011), which means any camera type no matter the cost could be used to do field measurements. In addition, digital photos can be stored. Thus the LAD result can always be checked again whenever it is needed. The photos also provide more information about the maize canopy such as the health status, which can be checked directly from the photo. If measurement is done across developing stages, the DP method would record the growth of the crop leaves at the same time, which is also valuable information. One limitation of the DP method is that it cannot measure orientation in the azimuth direction. However, this would not be a problem for smartphone cameras, as the integrated magnetometer sensor inside the smartphone allows the user to tell orientation accurately. The leaf azimuth angle therefore could be measured easily.

de Wit suggested that about 400 leaves (when the leaves of the crop are flat) or leaf sections (when plant leaves are bent, for example, as with maize crop) suffices to get reproducible distribution functions. The presented A-D test results about the minimum sample size shows about 15 plants, 113 leaves or 300 measured leaf sections are adequate for the DP method. However, it has to be mentioned that the majority of the measured maize plants in this study only have 7 to 10 good leaves available for measurement, and therefore fewer leaves contribute to the acquisition of the LAD. It is not presented in de Wit's work (1965) how many maize plants, leaves and sections have been measured to calculate LAD and determine the required sample size. Pisek et al. (2013) claims that 75 measured leaves across the canopy of temperate and boreal tree species are sufficient to reliably obtain LAD at whole tree level based on the DP method, although Kucharik (Kucharik, M. Norman, & T. Gower, 1998) suggests in his work hundreds of leaves need to be measured. The inconsistent suggestion of minimum sample

size is also found in maize, as España et al. (1999) concluded that 24 maize plants would provide an accurate and representative LIDF. However, they drew the conclusion according to the study of a 3D architecture model of maize instead of using real canopy measurements. Therefore, further investigation is needed to quantify the minimum sample size.

5. Conclusions and recommendations

LAI and LAD are two important canopy structure variables for studying vegetation photosynthesis, evapotranspiration, and a number of other microclimate activities in ecosystems. Additionally, they are input parameters of many powerful models that simulate the radiation transfer and ecosystem functions. The LAI ground measurements are often done with instruments based on optical theory using the gap fraction model, and the LAD has to be quantified first in order to use the model. LAD is difficult to quantify due to its complexity, and it varies across growing stages, among and within species and cultivars and may be affected by the surrounding environment. The assumed LIDFs sometimes deviate from real canopy structure and introduce certain amounts of errors to LAI retrieval. Furthermore, the field measurement of LAD requires large amounts of work and time. The presented study investigated the LAD of maize plants, LAI retrieval performance using different LIDFs and a modified DP method to measure LAD. The following conclusions and recommendations are given:

In this study, the LAD of maize plants in vegetative and late reproductive stages is the plagiophile canopy type. The LAD of maize plants in the same reproductive stage but having different heights due to different environmental conditions does not significantly differ from each other, even though the mean leaf inclination angle increases 2°-3° as the height increases. The environmental conditions, soil type and water logging, do not affect LAD of maize canopy significantly.

Besides plagiophile type, planophile type canopy was also observed in this study. The reflectance of planophile type in R, G and NIR is higher than plagiophile type regardless of LAI level, and so is NDVI value at low LAI levels. The LAD has a big influence on bi-directional reflectance; therefore, one needs to be aware of it when using optical remote sensing imagery to derive LAI.

The presented canopy type cannot be generalized because the samples measured in the study generally have only 7-10 leaves available instead of the 15-21 that will give the full description of maize canopy. Therefore, it is recommended to mark the maize plants and measure the same plants during several key development stages. The A-D test has to be used with insights and awareness of sample size variation.

The study confirms that two-parameter LIDFs outperform single parameter LIDFs and the solution-improved trigonometric function gives the best fit among all LIDFs. In addition, the ellipsoidal distribution and rotated-ellipsoidal distribution fit better in planophile canopy type than in plagiophile type, and they are more capable of predicting planophile and erectophile canopy types. The trigonometric function is highly recommended to be applied to simulate LAD because of its good and robust performance. LAI could be accurately retrieved to some degree using parametric LIDFs or a non-parametric LIDF that best approximates the real LAD. However, to further validate the conclusion, it is recommended to use comparison with a direct LAI measurement result.

The DP method shows effectiveness and advantages in obtaining LAD. LAD from the DP method and manual measurements are not significantly different in this study. Therefore, the adjusted DP method

could produce reliable LAD measurements for maize canopy. The minimum sample needed for the DP method to generate a reproducible result is 15 plants and 113 leaves. But this only applies to the sampled maize field. There is no consistent agreement about the minimum sample size yet, thus further investigation is needed. The DP method in this study could be easily applied to maize plants that have a full canopy structure.

The DP method has a number of advantages compared to the previous LAD measurement methods: it is portable, affordable and flexible with more efficiency; it could store the LAD information for reuse; and it records more information about the measured plants. It can be easily incorporated into a smartphone platform. Together with the other integrated sensors, it is possible to measure leaf orientation in an azimuth direction. This suggests a significant potential for sampling LAD and in turn LAI using smartphones.

References

Baret, F., de Solan, B., Lopez-Lozano, R., Ma, K., & Weiss, M. (2010). GAI estimates of row crops from downward looking digital photos taken perpendicular to rows at 57.5° zenith angle: Theoretical considerations based on 3D architecture models and application to wheat crops. *Agricultural and Forest Meteorology*, *150*(11), 1393–1401. doi:10.1016/j.agrformet.2010.04.011

Baret, F., Hagolle, O., Geiger, B., Bicheron, P., Miras, B., Huc, M., … Leroy, M. (2007). LAI, fAPAR and fCover CYCLOPES global products derived from VEGETATION. *Remote Sensing of Environment*, *110*(3), 275–286. doi:10.1016/j.rse.2007.02.018

Bonhomme, R., Grancher, C. V., & Chartier, P. (1974). use of hemispherical photographs for determining the leaf area index of young crops. *Photosynthetica*. Retrieved from http://agris.fao.org/agris-search/search.do?recordID=US201303086680

Bréda, N. J. J. (2003). Ground-based measurements of leaf area index: a review of methods, instruments and current controversies. *Journal of Experimental Botany*, *54*(392), 2403–17. doi:10.1093/jxb/erg263

Broge, N. H., & Leblanc, E. (2001). Comparing prediction power and stability of broadband and hyperspectral vegetation indices for estimation of green leaf area index and canopy chlorophyll density, *76*(2000), 156–172.

Campbell, G. S. (1986). Extinction coefficients for radiation in plant canopies calculated using an ellipsoidal inclination angle distribution. *Agricultural and Forest Meteorology*, *36*(4), 317–321. doi:10.1016/0168-1923(86)90010-9

Chen, J. M., & Black, T. A. (1991). Measuring leaf area index of plant canopies with branch architecture. *Agricultural and Forest Meteorology*, *57*(1-3), 1–12. doi:10.1016/0168-1923(91)90074-Z

Confalonieri, R., Foi, M., Casa, R., Aquaro, S., Tona, E., Peterle, M., … Acutis, M. (2013). Development of an app for estimating leaf area index using a smartphone. Trueness and precision determination and comparison with other indirect methods. *Computers and Electronics in Agriculture*, *96*, 67–74. doi:10.1016/j.compag.2013.04.019

Darvishzadeh, R., Skidmore, A., Schlerf, M., Atzberger, C., Corsi, F., & Cho, M. (2008). LAI and chlorophyll estimation for a heterogeneous grassland using hyperspectral measurements. *ISPRS Journal of Photogrammetry and Remote Sensing*, *63*(4), 409–426. doi:10.1016/j.isprsjprs.2008.01.001

Demarez, V., Duthoit, S., Baret, F., Weiss, M., & Dedieu, G. (2008). Estimation of leaf area and clumping indexes of crops with hemispherical photographs. *Agricultural and Forest Meteorology*, *148*(4), 644–655. doi:10.1016/j.agrformet.2007.11.015

España, M., Baret, F., Aries, F., Andrieu, B., & Chelle, M. (1999). Radiative transfer sensitivity to the accuracy of canopy structure description. The case of a maize canopy. *Agronomie*, *19*(3-4), 241–254. doi:10.1051/agro:19990305

Flerchinger, G. N., & Yu, Q. (2007). Simplified expressions for radiation scattering in canopies with ellipsoidal leaf angle distributions. *Agricultural and Forest Meteorology*, *144*(3-4), 230–235. doi:10.1016/j.agrformet.2007.03.002

Frasson, R. P. D. M., & Krajewski, W. F. (2010). Three-dimensional digital model of a maize plant. *Agricultural and Forest Meteorology*, *150*(3), 478–488. doi:10.1016/j.agrformet.2010.01.003

Goel, N. S., & Strebel, D. E. (1984). (1984) Simple Beta Distribution Representation of Leaf Orientation in Vegetation Canopies (AJ).

Goudriaan, J. (1988). The bare bones of leaf-angle distribution in radiation models for canopy photosynthesis and energy exchange. *Agricultural and Forest Meteorology*, *43*(2), 155–169. doi:10.1016/0168-1923(88)90089-5

Gupta, A. K., & Nadarajah, S. (2004). *Handbook of Beta Distribution and Its Applications*. (A. K. Gupta & S. Nadarajah, Eds.). Retrieved from https://books.google.com/books?hl=nl&lr=&id=cVmnsxa-VzwC&pgis=1

Haboudane, D. (2004). Hyperspectral vegetation indices and novel algorithms for predicting green LAI of crop canopies: Modeling and validation in the context of precision agriculture. *Remote Sensing of Environment*, *90*(3), 337–352. doi:10.1016/j.rse.2003.12.013

Homem Antunes, M. A., Walter-Shea, E. A., & Mesarch, M. A. (2001). Test of an extended mathematical approach to calculate maize leaf area index and leaf angle distribution. *Agricultural and Forest Meteorology*, *108*(1), 45–53. doi:10.1016/S0168-1923(01)00219-2

Hosoi, F., Nakabayashi, K., & Omasa, K. (2011). 3-D modeling of tomato canopies using a high-resolution portable scanning lidar for extracting structural information. *Sensors (Basel, Switzerland)*, *11*(2), 2166–74. doi:10.3390/s110202166

Hosoi, F., & Omasa, K. (2009). Estimating vertical plant area density profile and growth parameters of a wheat canopy at different growth stages using three-dimensional portable lidar imaging. *ISPRS Journal of Photogrammetry and Remote Sensing*, *64*(2), 151–158. doi:10.1016/j.isprsjprs.2008.09.003

Knyazikhin, Y., Schull, M. A., Stenberg, P., Mõttus, M., Rautiainen, M., Yang, Y., … Myneni, R. B. (2013). Hyperspectral remote sensing of foliar nitrogen content. *Proceedings of the National Academy of Sciences of the United States of America*, *110*(3), E185–92. doi:10.1073/pnas.1210196109

Kucharik, C. J., M. Norman, J., & T. Gower, S. (1998). Measurements of leaf orientation, light distribution and sunlit leaf area in a boreal aspen forest. *Agricultural and Forest Meteorology*, *91*(1-2), 127–148. doi:10.1016/S0168-1923(98)00058-6

Lang, A. R. G. (1973). Leaf orientation of a cotton plant. *Agricultural Meteorology*, *11*, 37–51. doi:10.1016/0002-1571(73)90049-6

Lemeur, R. (1973). A method for simulating the direct solar radiation regime in sunflower, jerusalem artichoke, corn and soybean canopies using actual stand structure data. *Agricultural Meteorology*, *12*(3598), 229–247. doi:10.1016/0002-1571(73)90022-8

Liu, J., Pattey, E., & Admiral, S. (2013). Assessment of in situ crop LAI measurement using unidirectional view digital photography. *Agricultural and Forest Meteorology*, *169*, 25–34. doi:10.1016/j.agrformet.2012.10.009

Loomis, R. S., Williams, W. A., Duncan, W. G., Dovrat, A., & Nunez A., F. (1968). Quantitative Descriptions of Foliage Display and Light Absorption in Field Communities of Corn Plants1. *Crop Science*, *8*(3), 352. doi:10.2135/cropsci1968.0011183X000800030027x

Maddonni, G. A., & Otegui, M. E. (1996). Leaf area, light interception, and crop development in maize. *Field Crops Research*, *48*(1), 81–87. doi:10.1016/0378-4290(96)00035-4

Maddonni, G. A., Otegui, M. E., Andrieu, B., Chelle, M., & Casal, J. J. (2002). Maize leaves turn away from neighbors. *Plant Physiology*, *130*(3), 1181–9. doi:10.1104/pp.009738

Nichiporovich, A. A. (1961). Properties of plant crops as an optical system. *Soviet Pl. Physiol*, *8*, 428–435.

Nilson, T. (1971). A theoretical analysis of the frequency of gaps in plant stands. *Agricultural Meteorology*, *8*, 25–38. doi:10.1016/0002-1571(71)90092-6

Omasa, K., Hosoi, F., & Konishi, A. (2007). 3D lidar imaging for detecting and understanding plant responses and canopy structure. *Journal of Experimental Botany*, *58*(4), 881–98. doi:10.1093/jxb/erl142

Pisek, J., Ryu, Y., & Alikas, K. (2011). Estimating leaf inclination and G-function from leveled digital camera photography in broadleaf canopies. *Trees*, *25*(5), 919–924. doi:10.1007/s00468-011-0566-6

Pisek, J., Sonnentag, O., Richardson, A. D., & Mõttus, M. (2013). Is the spherical leaf inclination angle distribution a valid assumption for temperate and boreal broadleaf tree species? *Agricultural and Forest Meteorology*, *169*, 186–194. doi:10.1016/j.agrformet.2012.10.011

Propastin, P., & Panferov, O. (2013). Retrieval of remotely sensed LAI using Landsat ETM+ data and ground measurements of solar radiation and vegetation structure: Implication of leaf inclination angle. *International Journal of Applied Earth Observation and Geoinformation*, *25*, 38–46. doi:10.1016/j.jag.2013.02.006

Rex, A. (2010). *Determination of nutrient composition of mangroves through combined statistical and physical modeling*. ITC, University of Twente.

Ross, I. (1981). *The radiation regime and architecture of plant stands*. Springer Science & Business Media. Retrieved from http://books.google.com/books?id=w6SogqDOa54C&pgis=1

Ryu, Y., Sonnentag, O., Nilson, T., Vargas, R., Kobayashi, H., Wenk, R., & Baldocchi, D. D. (2010). How to quantify tree leaf area index in an open savanna ecosystem: A multi-instrument and multi-model approach. *Agricultural and Forest Meteorology*, *150*(1), 63–76. doi:10.1016/j.agrformet.2009.08.007

Sandmann, M., Graefe, J., & Feller, C. (2013). Optical methods for the non-destructive estimation of leaf area index in kohlrabi and lettuce. *Scientia Horticulturae*, *156*, 113–120. doi:10.1016/j.scienta.2013.04.003

Scholz, F. W., & Stephens, M. a. (1987). K-Sample Anderson-Darling Tests. *Journal of the American Statistical Association*, *82*(399), 918–924. doi:10.1080/01621459.1987.10478517

Shell, G. S. G., Lang, A. R. G., & Sale, P. J. M. (1974). Quantitative measures of elaf orientation and heliotropic reponse in sunflower, bean, pepper and cucumber, *13*, 25–37.

Smith, B., Knorr, W., Widlowski, J.-L., Pinty, B., & Gobron, N. (2008). Combining remote sensing data with process modelling to monitor boreal conifer forest carbon balances. *Forest Ecology and Management*, *255*(12), 3985–3994. doi:10.1016/j.foreco.2008.03.056

Stewart, D. W., & Dwyer, L. M. (1993). Mathematical characterization of maize canopies. *Agricultural and Forest Meteorology*, *66*(3-4), 247–265. doi:10.1016/0168-1923(93)90074-R

Stewart, D. W., & Dwyer, L. M. (1999). Mathematical Characterization of Leaf Shape and Area of Maize Hybrids. *Crop Science*, *39*(2), 422. doi:10.2135/cropsci1999.0011183X0039000200021x

Thomas, S. C., & Winner, W. E. (2000). A rotated ellipsoidal angle density function improves estimation of foliage inclination distributions in forest canopies. *Agricultural and Forest Meteorology*, *100*(1), 19–24. doi:10.1016/S0168-1923(99)00089-1

Trujillo-Ortiz, A., Hernandez-Walls, R., Barba-Rojo, K., Cupul-Magana, L., & Zavala-Garcia, R. C. (2007). AnDarksamtest:Anderson-Darling k-sample procedure to test the hypothesis that the populations of the drawned groups are identical. Retrieved from http://www.mathworks.com/matlabcentral/fileexchange/loadFile.do?objectId=17451

Verhoef, W. (1997). *Theory of radiative transfer models applied in optical remote sensing of vegetation canopies*.

Verhoef, W., & Bach, H. (2007). Coupled soil-leaf-canopy and atmosphere radiative transfer modeling to simulate hyperspectral multi-angular surface reflectance and TOA radiance data. *Remote Sensing of Environment*, *109*, 166–182. doi:10.1016/j.rse.2006.12.013

Verhoef, W., & Bunnik, N. J. J. (1975). *A Model Study on the Relations Between Crop Characteristics and Canopy Spectral Reflectance: 1. Deduction of Crop Parameters from Canopy Spectroreflectance Data: 2. Detectability of Variations in Crop Parameters by Multispectral Scanning*.

Wang, W.-M., Li, Z.-L., & Su, H.-B. (2007). Comparison of leaf angle distribution functions: Effects on extinction coefficient and fraction of sunlit foliage. *Agricultural and Forest Meteorology*, *143*(1-2), 106–122. doi:10.1016/j.agrformet.2006.12.003

Wang, Y. P., & Jarvis, P. G. (1988). Mean leaf angles for the ellipsoidal inclination angle distribution. *Agricultural and Forest Meteorology*, *43*(3-4), 319–321. doi:10.1016/0168-1923(88)90057-3

Warren-Wilson, J. (1963). Estimation of foliage denseness and foliage angle by inclined point quadrats. *Australian Journal of Botany*, *11*, 95–105.

Weiss, M. (1991). *VALERI: Deriving leaf area index and average leaf inclination angle from LAI2000 Measurements*. ----------. Retrieved from http://w3.avignon.inra.fr/valeri/methodology/LAI2000INRADoc.pdf

Weiss, M., & Baret, F. (2014). CAN-EYE V6.313 User Manual, (May).

Weiss, M., Baret, F., Smith, G. J., Jonckheere, I., & Coppin, P. (2004). Review of methods for in situ leaf area index (LAI) determination. *Agricultural and Forest Meteorology*, *121*(1-2), 37–53. doi:10.1016/j.agrformet.2003.08.001

Weligepolage, K., Gieske, A. S. M., & Su, Z. (2012). Surface roughness analysis of a conifer forest canopy with airborne and terrestrial laser scanning techniques. *International Journal of Applied Earth Observation and Geoinformation*, *14*(1), 192–203. doi:10.1016/j.jag.2011.08.014

Wilson, J. W. (1960). INCLINED POINT QUADRATS. *New Phytologist*, *59*(1), 1–7. doi:10.1111/j.1469-8137.1960.tb06195.x

Wilson, J. W. (1967). STAND STRUCTURE AND LIGHT PENETRATION. *Journal of Applied Ecology*, *4*(1), 159–165. Retrieved from http://www.jstor.org/discover/10.2307/2401415?uid=40855&uid=3738736&uid=2&uid=3&uid=67&uid=5911848&uid=40854&uid=62&sid=21104653694093

Wit, C. T. de. (1965, December 2). Photosynthesis of leaf canopies. Pudoc. Retrieved from http://edepot.wur.nl/187115

ZHANG, X., LU, C., HU, N., YAO, K., ZHANG, Q., & DAI, Q. (2013). Simulation of Canopy Leaf Inclination Angle in Rice. *Rice Science*, *20*(6), 434–441. doi:10.1016/S1672-6308(13)60161-4

Zheng, G., & Moskal, L. M. (2009). Retrieving Leaf Area Index (LAI) Using Remote Sensing: Theories, Methods and Sensors. *Sensors (Basel, Switzerland)*, *9*(4), 2719–45. doi:10.3390/s90402719

Zheng, G., & Moskal, L. M. (2012). Spatial variability of terrestrial laser scanning based leaf area index. *International Journal of Applied Earth Observation and Geoinformation*, *19*, 226–237. doi:10.1016/j.jag.2012.05.002

Zou, X., & Mõttus, M. (2015). Retrieving crop leaf tilt angle from imaging spectroscopy data. *Agricultural and Forest Meteorology*, *205*, 73–82. doi:10.1016/j.agrformet.2015.02.016

Zou, X., Mõttus, M., Tammeorg, P., Torres, C. L., Takala, T., Pisek, J., … Pellikka, P. (2014). Photographic measurement of leaf angles in field crops. *Agricultural and Forest Meteorology*, *184*, 137–146. doi:10.1016/j.agrformet.2013.09.010

Appendix

Table 17 LAD of 6 categories from manual measurement

Bin	category 1		category 2		category 3		category 4		category 5		category 6	
	Area count	Freq-uency	Area count	Freq-uency	Area count	Freq-uency	Area count	Freq-uency	Area count	Freq-uency	Area count	Freq-uency
0-5	47.4214	0.0103	782.8280	0.0204	289.8172	0.0081	513.5691	0.0091	341.3371	0.0063	455.0948	0.0394
5-10	261.0406	0.0568	1740.3332	0.0453	1258.5962	0.0353	1807.4650	0.0321	2665.8404	0.0491	1625.4501	0.1409
10-15	116.6120	0.0254	1676.1881	0.0437	1701.3940	0.0478	2906.9069	0.0517	2275.3367	0.0419	1030.0585	0.0893
15-20	246.9785	0.0538	2128.7924	0.0555	1410.7981	0.0396	1291.4976	0.0230	1601.8974	0.0295	1866.7038	0.1618
20-25	187.7424	0.0409	2155.2565	0.0562	1819.7648	0.0511	2320.4376	0.0412	2614.9726	0.0481	1324.2023	0.1148
25-30	293.1049	0.0638	2271.2109	0.0592	1723.4888	0.0484	2342.9718	0.0416	1746.0490	0.0321	1051.9305	0.0912
30-35	391.7376	0.0853	2588.5512	0.0674	2887.4709	0.0811	4613.5285	0.0820	2591.2515	0.0477	1236.7513	0.1072
35-40	390.0793	0.0849	4025.7212	0.1049	1985.5915	0.0557	2185.2216	0.0388	1895.6305	0.0349	1207.1186	0.1046
40-45	725.0701	0.1578	6375.0389	0.1661	3546.2464	0.0996	4299.2709	0.0764	3621.3733	0.0667	689.5457	0.0598
45-50	519.9922	0.1132	4376.9396	0.1140	4619.8979	0.1297	4593.7623	0.0817	6537.7951	0.1204	549.8880	0.0477
50-55	401.0882	0.0873	3723.9725	0.0970	4979.1066	0.1398	7601.4690	0.1351	5288.2930	0.0974	98.3900	0.0085
55-60	346.2923	0.0754	2231.7902	0.0581	4137.2657	0.1161	7811.3788	0.1388	5067.5623	0.0933	0.0000	0.0000
60-65	332.9152	0.0725	1549.1958	0.0404	3903.6596	0.1096	8371.3956	0.1488	5808.9704	0.1070	198.8925	0.0172
65-70	209.5647	0.0456	895.1714	0.0233	704.8354	0.0198	3557.9248	0.0632	5333.8473	0.0982	84.8406	0.0074
70-75	32.0412	0.0070	217.2244	0.0057	431.1693	0.0121	1028.9637	0.0183	3723.1148	0.0685	69.0167	0.0060
75-80	18.5114	0.0040	474.9215	0.0124	36.2847	0.0010	597.3877	0.0106	2438.3029	0.0449	48.1266	0.0042
80-85	65.7378	0.0143	663.5289	0.0173	133.8757	0.0038	315.6549	0.0056	412.8853	0.0076	0.0000	0.0000
85-90	7.7200	0.0017	505.7360	0.0132	50.7861	0.0014	102.8617	0.0018	348.3640	0.0064	0.0000	0.0000
Sum	**4593.6500**	1.0000	**38382.4008**	1.0000	**35620.0488**	1.0000	**56261.6675**	1.0000	**54312.8238**	1.0000	**11536.0100**	1.0000

Table 18 LAD of 5 categories from DP method

Bin	category 1		category 2		category 3		category 4		category 6	
	Area count	Frequency	Area count	Frequency	Area count	Frequency	Area count	Frequency	Area count	Frequency
0-5	120.7840	0.0278	863.5100	0.0253	1560.5403	0.0449	1598.5341	0.0331	1056.5989	0.1001
5-10	257.8380	0.0594	3259.2159	0.0955	2159.6880	0.0621	2579.8372	0.0534	845.3656	0.0801
10-15	279.1759	0.0643	1978.2292	0.0580	2069.2398	0.0595	1712.9339	0.0355	1271.7481	0.1205
15-20	284.9039	0.0656	1598.0388	0.0468	2252.4704	0.0647	1791.1077	0.0371	1767.3353	0.1674
20-25	271.0127	0.0624	2001.0965	0.0586	2101.4791	0.0604	1752.2219	0.0363	1296.3614	0.1228
25-30	342.8685	0.0790	2185.9696	0.0641	1590.4744	0.0457	2972.2416	0.0615	994.4121	0.0942
30-35	393.0168	0.0905	2685.5960	0.0787	1787.1099	0.0514	2653.5009	0.0549	1289.1519	0.1221
35-40	387.7618	0.0893	4821.0585	0.1413	2228.0463	0.0640	2721.0509	0.0563	742.8311	0.0704
40-45	507.6859	0.1169	3951.0115	0.1158	2721.9593	0.0782	2616.4876	0.0542	593.7470	0.0562
45-50	529.6004	0.1220	2616.5067	0.0767	3666.3365	0.1054	4230.6248	0.0876	379.7146	0.0360
50-55	463.2922	0.1067	3948.8198	0.1157	5051.6995	0.1452	5092.7573	0.1054	81.8411	0.0078
55-60	143.3459	0.0330	2201.0966	0.0645	3640.8860	0.1046	5864.8486	0.1214	34.4511	0.0033
60-65	173.5699	0.0400	835.6430	0.0245	1567.0102	0.0450	7255.5402	0.1502	91.9225	0.0087
65-70	76.2220	0.0176	326.1139	0.0096	1818.7383	0.0523	3906.2012	0.0809	80.8821	0.0077
70-75	69.3599	0.0160	166.3483	0.0049	253.7767	0.0073	1156.2590	0.0239	0.0239	0.0000
75-80	10.6010	0.0024	313.8143	0.0092	100.8948	0.0029	106.7096	0.0022	29.6722	0.0028
80-85	8.0631	0.0019	78.0789	0.0023	38.0922	0.0011	245.7177	0.0051	0.0051	0.0000
85-90	22.1622	0.0051	289.4660	0.0085	183.7724	0.0053	56.3724	0.0012	0.0012	0.0000
Sum	4341.2639	1.0000	34119.6135	1.0000	34792.2142	1.0000	48312.9466	1.0000	10556.0654	1.0000

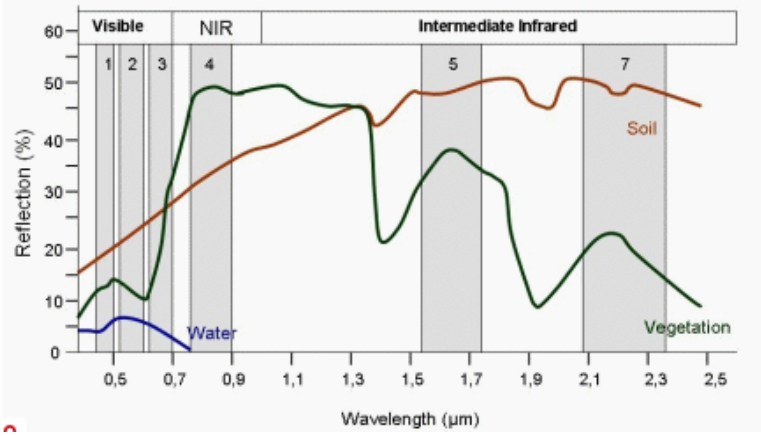

Figure 25 The reflectance property of vegetation and soil[3]

Figure 26 Study field for category 1 – 6 and the planophile looking maize plant (a) category 1 (b) category 2 (c) category 3-6 (d) planophile looking plant in category 6

[3] The figure is from SEOS project http://www.seos-project.eu/modules/remotesensing/remotesensing-c01-p05.html

Figure 27 Water logging and loam soil effect in category 2 and black soil in category 5

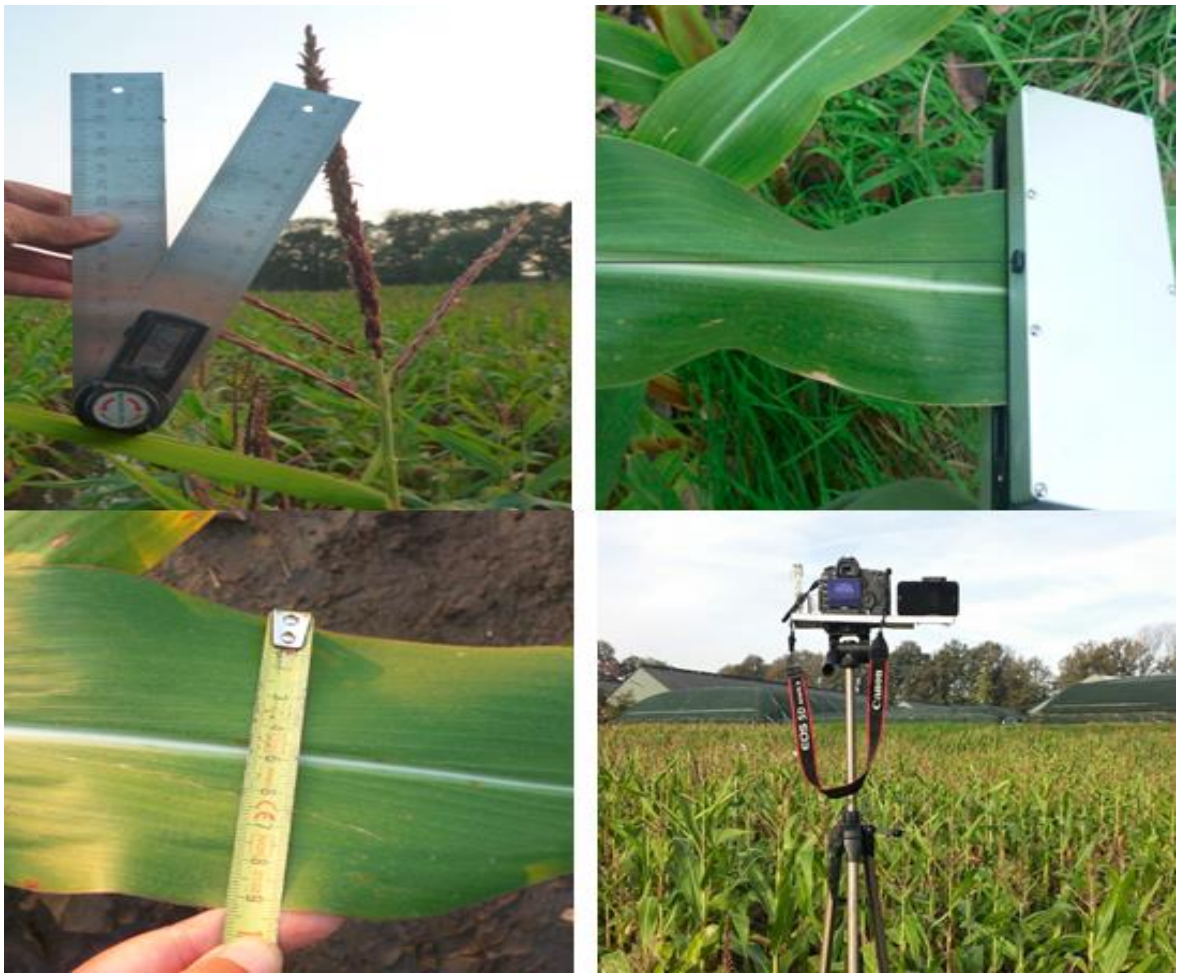

Figure 28 Demonstration of leaf inclination angle, leaf area, leaf width and gap fraction measurement